Journal of Medicinal Chemistry

Drug Annotation

Discovery of (*R*)-6-(1-(8-fluoro-6-(1-methyl-1*H*-pyrazol-4-yl)-[1,2,4]triazolo[4,3-*a*]pyridin-3-yl)ethyl)-3-(2-methoxyethoxy)-1,6-naphthyridin-5(6*H*)-one (AMG 337), a Potent and Selective Inhibitor of MET with High Unbound Target Coverage and Robust *In Vivo* Antitumor Activity

Alessandro A Boezio, Katrina W Copeland, Karen Rex, Brian K Brian K. Albrecht, David Bauer, Steve F Bellon, Christiane Bode, Martin A Broome, Deborah Choquette, Angela Coxon, Isabelle Dussault, Satoko Hirai, Richard T. Lewis, Min-Hwa Jasmine Lin, Julia Lohman Suchomel, Jingzhou Liu, Emily A Peterson, Michele Potashman, Roman Shimanovich, Yohannes Teffera, Douglas A. Whittington, Karina R Vaida, and Jean-Christophe Harmange

J. Med. Chem., **Just Accepted Manuscript** • DOI: 10.1021/acs.jmedchem.5b01716 • Publication Date (Web): 26 Jan 2016

ACS Publications

Journal of Medicinal Chemistry is published by the American Chemical Society. 1155 Sixteenth Street N.W., Washington, DC 20036

Discovery of (*R*)-6-(1-(8-fluoro-6-(1-methyl-1*H*-pyrazol-4-yl)-[1,2,4]triazolo[4,3-*a*]pyridin-3-yl)ethyl)-3-(2-methoxyethoxy)-1,6-naphthyridin-5(6*H*)-one (AMG 337), a Potent and Selective Inhibitor of MET with High Unbound Target Coverage and Robust *In Vivo* Antitumor Activity

Alessandro A. Boezio,[*,†] Katrina W. Copeland,[†] Karen Rex,[‡] Brian K. Albrecht,[†] David Bauer,[†] Steven F. Bellon,[†] Christiane Boezio,[†] Martin A. Broome,[‡] Deborah Choquette,[†] Angela Coxon,[‡] Isabelle Dussault,[‡] Satoko Hirai,[†] Richard Lewis,[†] Min-Hwa Jasmine Lin,[†] Julia Lohman,[†] Jingzhou Liu,[†] Emily A. Peterson,[†] Michele Potashman,[†] Roman Shimanovich,[†] Yohannes Teffera,[†] Douglas A. Whittington,[†] Karina R. Vaida[†] and Jean-Christophe Harmange[†]

†Amgen Inc., 360 Binney Street, Cambridge, Massachusetts 02142, United States

‡Amgen Inc., One Amgen Center Drive, Thousand Oaks, California 91320, United States

KEYWORDS: MET, oncology, naphthyridinone

ABSTRACT: Deregulation of the receptor tyrosine kinase mesenchymal epithelial transition factor (MET) has been implicated in several human cancers and is an attractive target for small molecule drug discovery. Herein, we report the discovery of compound **23** (AMG 337), which demonstrates nanomolar inhibition of MET kinase activity, desirable pre-clinical pharmacokinetics, significant inhibition of MET phosphorylation in mice and robust tumor growth inhibition in a MET-dependent mouse efficacy model.

MANUSCRIPT TEXT:

Introduction

The receptor tyrosine kinase MET and hepatocyte growth factor (HGF), its endogenous ligand, are implicated in several cellular processes relevant to cancer, including cell proliferation, cell migration and invasive growth. These also play an important role in embryonic development and wound healing.[1]

However, deregulation of the MET/HGF pathway can lead to tumorigenesis and metastasis.[2] Amplification of the MET gene, overexpression of MET and/or HGF and constitutive activation conferred by sequence mutations are some of the mechanisms of deregulation found in human cancers.[3]

Several approaches to inhibiting the HGF/MET pathway are currently being tested in the clinic.[4] The appeal of an ATP-competitive, small molecule inhibitor acting via the intracellular kinase domain is based on its potential to block both ligand-dependent and ligand-independent activities of MET.[5] We previously reported the discovery of a potent, orally active MET inhibitor (Class II) for the treatment of cancer,[6] and more recently disclosed four distinct series (represented by **1**,[7] **2**,[8] **3**[9] and **4**[10], Table 1) of potent and uniquely selective MET inhibitors with a common u-shape binding mode (Class Ib). However, each series suffered from its own unique liabilities. Efforts to improve upon these series led to the discovery of a naphthyridinone series of MET inhibitors (represented by **5**, Figure 1), leading to the discovery of **23**[11] (Table 3). Herein, we describe the design, synthesis, pharmacokinetics and *in vivo* efficacy of this class of compounds.

Results and Discussion

The previously reported compounds (**1-4**)[7-10] all show impressive enzymatic and cellular MET potencies. Compound **1**, in the *O*-linked series, was the first of the U-shaped inhibitors disclosed. **1** exhibited single-digit nanomolar potency in our cellular assay, suitable PK, and showed >90% inhibition of HGF-induced phosphorylation of MET in a mouse liver pharmacodynamic (PD) model for up to 6 h (*vide infra*). However, this series was later found to exhibit time-dependent inhibition (TDI) of CYP3A4.[12] To overcome this liability, the *N*-linked series represented by compound **2** was developed. This series showed similar potency and *in vivo* tumor response to compound **1**, but no longer suffered from TDI. Despite the advances made in the *O*- and *N*-linked series, both suffered from poor solubility and shorter-than-desired duration of coverage in our PD model (>90% inhibition at 30 mg/kg up to 6 h was observed for both series).

Table 1. Representative MET compounds (**1-4**) from four distinct series

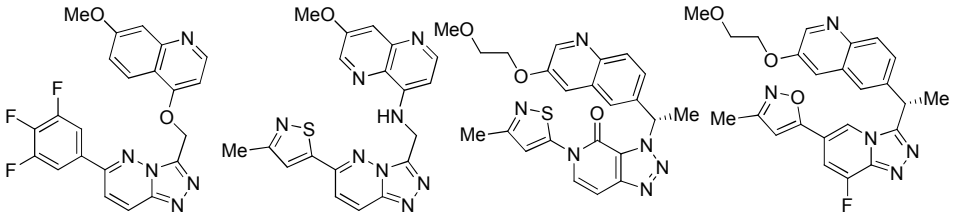

"*O*-Linked" "*N*-Linked" "Triazolopyridinone" "Triazolopyridine"

Compound	1	2	3	4
MET IC_{50}				
Biochemical[a]	4 nM	6 nM	0.6 nM	1 nM
Cellular[b]	8 nM	3 nM	2 nM	5 nM
LipE[c] (cLogP)	4.2 (4.2)	5.6 (2.6)	6.4 (2.8)	5.4 (3.5)
Solubility				
0.01 N HCl / PBS / SIF (μg/mL)	85 / 4 / 17	>200 / 3 / 13	37 / 9 / 40	>200 / 52 / 126
CYP3A4 TDI[d]				
IC_{50} / IC_{50} (w/Preinc.) (μM)	29 / 2.0	>50 / 26	21 / 1.5	>50 / >50
Rat pharmacokinetics[e]				
Cl (L/h/kg)	0.06[g]	0.19[i]	0.56[j]	0.57[j]
Cl_u (L/h/kg)[f]	58	26	31	26
F (%)	22[h]	31[h]	43[k]	46[k]
$T_{1/2}$ (h)	3.5	1.8	3.4	4.2
Liver PD response[l]				
Dose (mg/kg)	30	30	10	10
Last time pt >90% inhibition	6 h	6 h	12 h	6 h
Plasma C_u at time pt	34 nM	9 nM	20 nM	141 nM

[a]Inhibition of MET kinase activity, n ≥ 2. [b]Inhibition of HGF-mediated MET phosphorylation in PC3 cells, n ≥ 2. [c]LipE = pIC_{50} – clog P. [13,14] [d]Inhibition of CYP3A4 (midazolam 1'-hydroxylation) IC_{50} shift with and without pre-incubation of the compound in the presence of NADPH. [e]*In vivo* experiments were carried out with male Sprague-Dawley rats n = 3. [f]Unbound fraction (f_u) was measured using equilibrium dialysis; Concentration = 5 g/mL. [g]*iv*, 0.3 mg/kg (DMSO). [h]*po*, 2 mg/kg (2% hydroxypropyl methylcellulose 1% Tween 80 in water, pH 2.2 adjusted with hydrochloric acid). [i]*iv*, 0.25 mg/kg (20% hydroxypropyl beta-

cyclodextrin in water, pH 3.5 adjusted with methanesulfonic acid). [j]*iv*, 0.25 mg/kg (DMSO). [k]*po*, 2 mg/kg, (2% hydroxypropyl methylcellulose 1% Tween 80 in water, pH 2.2 adjusted with methanesulfonic acid). [l]See references 7, 8, 9 and 10 for PD measurements.

In an attempt to improve solubility and increase the *in vivo* exposure of **1** and **2**, compound **3** was designed *de novo* while maintaining the same key binding interactions with MET. Despite little improvement in solubility, this new series showed outstanding efficacy and extended coverage in a mouse PD model. This compound displayed >90% inhibition of HGF-induced phosphorylation of MET at 10 mg/kg up to 12 h, with an associated unbound plasma concentration of 20 nM providing 11-fold coverage of the cellular IC_{50}. As antitumor activity in a xenograft model (*vide infra*) was strongly correlated with high and extended inhibition in our PD model (>90% inhibition for >12 h) was preferable.[15] Upon further investigation, it was determined that this series of compounds unfortunately also suffered from TDI of CYP3A4. In a parallel investigation, the use of a triazolopyridine ring instead of a triazolopyridinone ring led to the identification of **4**, which maintained potency and did not exhibit TDI liabilities while displaying good solubility. However, **4** suffered from lesser sustained efficacy in the PD model relative to compound **3**.

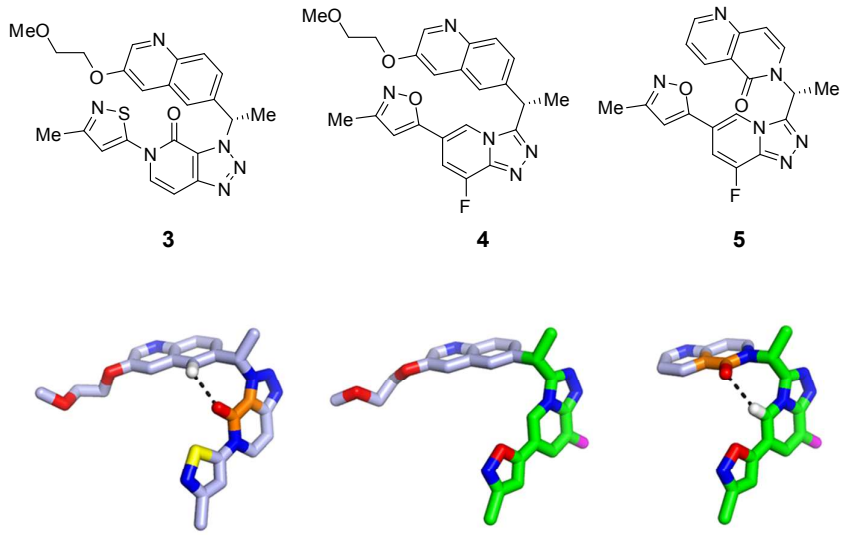

Figure 1. Origin of the naphthyridinone series, represented by hybrid **5**

In order to merge efficacy with mitigated TDI liability, two key design elements derived from **3** and **4** were hybridized to afford compound **5**. First, our attention was drawn to the superior efficacy of

compound **3** in the PD time-course model. We hypothesized that the favorable U-shaped binding-mode of **3** is reinforced by a key intramolecular interaction between the carbonyl of the pyridone and the hydrogen of the quinoline as shown in the Figure 1. Second, upon juxtaposition of **3** and **4**, we attributed the CYP3A4 TDI activity to the triazolopyridinone ring of **3**, since both series share a characteristic quinoline element. Accordingly, the fluorotriazolopyridine portion of **4** (in green), was combined with a naphthyridinone ring system to afford **5**, in which direction of the internal H-bond interaction, exhibited by **3**, has been reversed (in orange). This new scaffold was found to maintain single-digit nanomolar inhibition of MET phosphorylation (MET Biochemical IC_{50} 3 nM, Cellular IC_{50} 9 nM).

The synthesis of **5** required the individual construction of coupling partners **9a** and **13a** (Scheme 1). Stille cross-coupling of 5-chloro-2,3-difluoropyridine (**6**) and commercially available isoxazole stannane **7** yielded intermediate **8a**, which was treated with hydrazine to form pyridyl hydrazine **9a**. Coupling partner **13a** was prepared as a racemic mixture in two steps from naphthyridinone **10a** through alkylation with ethyl 2-bromopropanoate (**11**) followed by hydrolysis of the resultant ester (**12a**) under acidic conditions. Acid **13a** underwent HATU-mediated amide coupling with hydrazine **9a**, after which cyclization under dehydrative conditions provided the racemic fluorotriazolopyridine product in 52% yield over two steps. Finally, separation of racemic **5** by chiral chromatography afforded the active (*R*)-enantiomer of **5**.[16]

Scheme 1. Synthesis of **5**

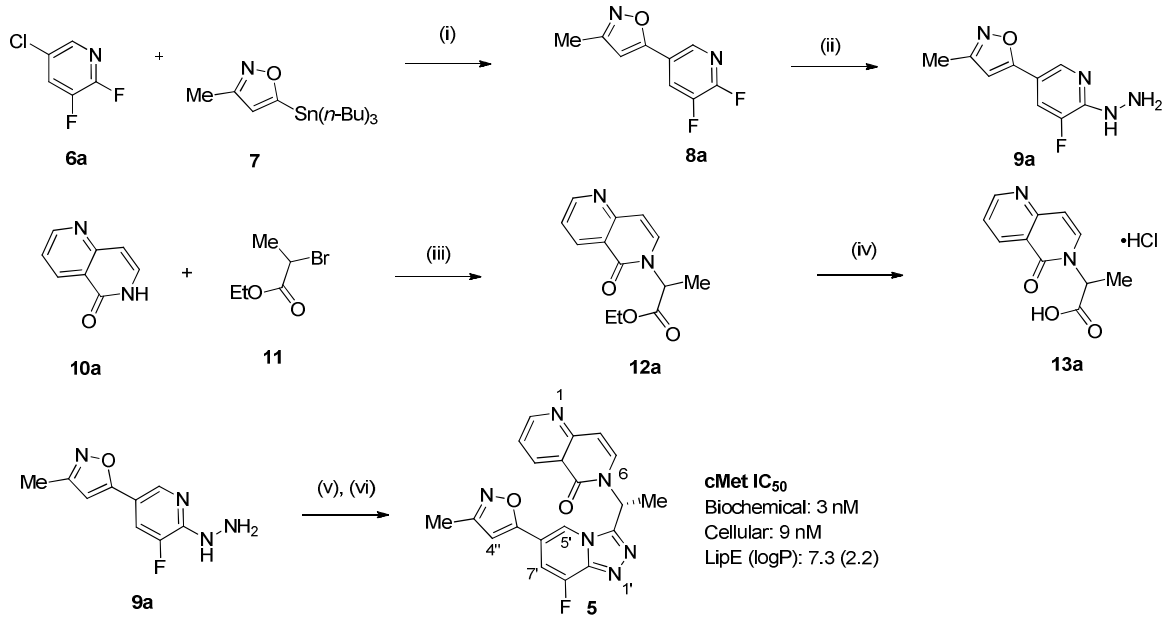

[a] Reagents and conditions: (i) $Pd(OAc)_2$, X-Phos, 1,4-dioxane/water, 100 °C, 18 h, 60%; (ii) NH_2NH_2, *i*-PrOH, 65 °C, 3 h, 90%; (iii) Cs_2CO_3, THF, 60 °C, 3 h, quantitative; (iv) aq. HCl, 60 °C, 7 h; (v) **13a**, HATU, Hunig's base, DMF, 23 °C, 3 h; (vi) PPh_3, $TMSN_3$, DEAD, THF, 23 °C, 3 h, 52% over two steps, then chiral separation.

Alternatively, an enantioselective synthesis of compound **5** was achieved via preparation of a chiral acid coupling partner **15** (Scheme 2).[17] Mitsunobu reaction between naphthyridinone **10a** and (*S*)-(-)-methyl lactate (**14**), followed by ester hydrolysis afforded compound **15** in high yield and >95% *ee*.[18] HATU mediated amide coupling of **9a** with **15**, followed by cyclization under dehydrative conditions yielded **5** in high yield and with complete retention of enantiomeric excess.

Scheme 2. Enantioselective synthesis of **5**

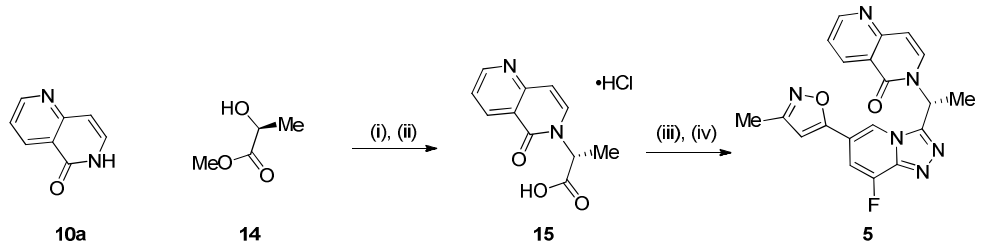

[a] Reagents and conditions: (i) PPh_3, DEAD, THF, 0 to 23 °C, 10 h; (ii) aq. HCl, THF, 75 °C, 10 h, 67% over two steps; (iii) **9a**, HATU, Hunig's base, MeCN, 0 °C, 30 min, 77%; (iv) PPh_3, $TMSN_3$, DEAD, THF, 20 °C, 1 h, 83%.

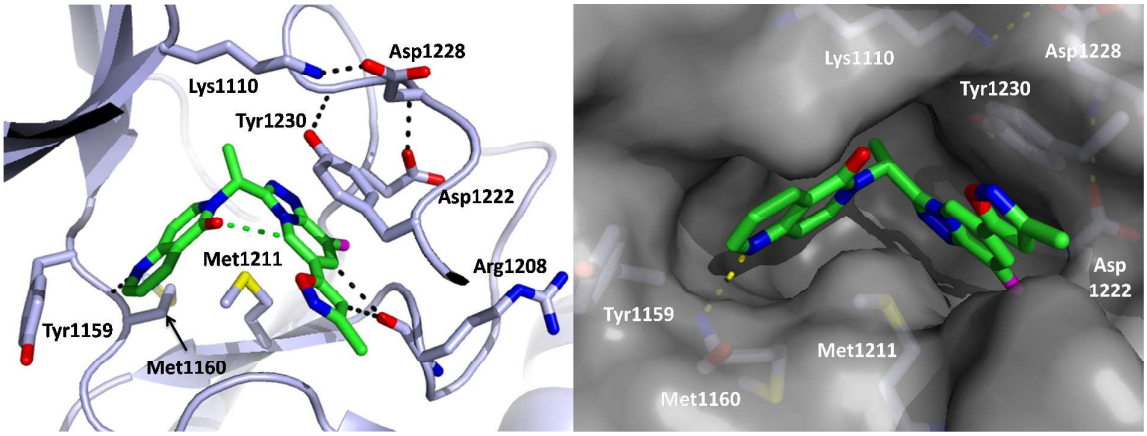

Figure 2. Co-crystal structure of MET and compound **5**

A co-crystal of **5** within the catalytic domain of unphosphorylated MET was obtained[19] (Figure 2) indicating that the inhibitor adopts the desired U-shaped binding mode around Met1211. Furthermore, Our hypothesis that the naphthyridinone carbonyl and H-5' of the fluorotriazolopyridine ring (3.3Å) would participate in an intramolecular H-bond to reinforce the optimal binding mode was confirmed. Figure 3 provides a 2D representation[20] of the key contacts made by **5** in the active-site of MET. The naphthyridinone nitrogen atom N-1 participates in a single-point hydrogen bond with linker residue Met1160, while N-1' of the fluorotriazolopyridine interacts with the backbone –NH of Asp 1222.[21] In addition, a face-to-face π-stacking interaction is observed between Tyr1230 and the fluorotriazolopyridine ring system. Furthermore, a two-point binding contact between C-7' and C-4'' and the lone pairs of the Arg1208 carbonyl group is apparent. Confirmation that the (*R*)-enantiomer is preferred by the protein was demonstrated by the methyl substituent filling a small, lipophilic pocket in MET, defined by the side chains of Val1092, Leu1157, Ala1226, and Lys1110.[22] Finally, the fluorine atom at the 8'-position fills a small cleft within the active site, where it sits perpendicular to the backbone carbonyl of Asn1209.

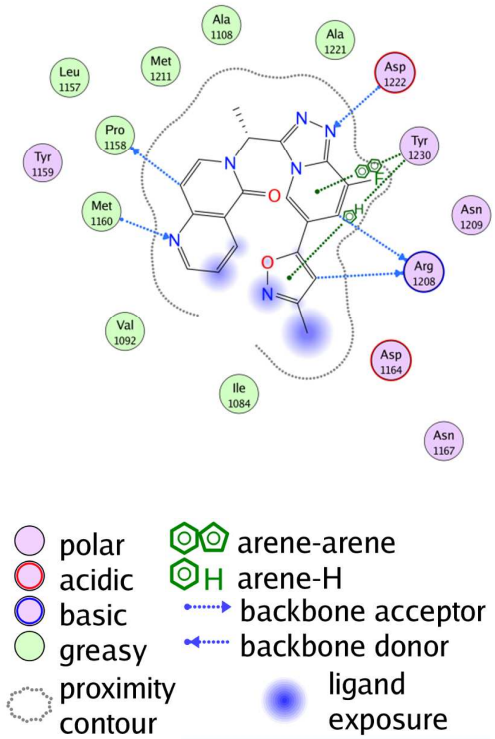

Figure 3. Ligand interaction diagram of MET and compound **5**

Having identified a structurally unique scaffold with nanomolar inhibition of MET phosphorylation we further characterized compound **5**. The solubility of **5** was superior to compounds **1**, **2** and **3** (0.01 N HCl / PBS / SIF (μg/mL): 172 / 34 / 55) and showed no time-dependent inhibition of CYP3A4 (pre-incubation IC_{50} >50 μM, post-incubation IC_{50} >50 μM). To supplement these promising data, the metabolic stability and pharmacokinetic properties of **5** were evaluated (Table 2). Compound **5** demonstrated low intrinsic clearance in rat, mouse and human liver microsomes. Additionally, the associated plasma free fraction (f_u) was high across species relative to compounds **1-4**. For example, rat free fraction for **1**: 0.001; **2**: 0.007; **3**: 0.018 and **4**: 0.022 in comparison to **5**: 0.196. Consistent with its low turnover in rat liver microsomes compound **5** was cleared at a low to moderate rate after dosing in male Sprague-Dawley rats. While **5** showed similar total clearance (Cl) to compounds **1-4** in rat, *i.e.* 0.38(L/h/kg) *vs* 0.06, 0.19, 0.56 and 0.57(L/h/kg) respectively, the unbound clearance (Cl_u) was significantly improved for **5** compare to **1-4** (1.9 (L/h/kg) *vs* 58, 26, 31, and 26 (L/h/kg) respectively), which could be advantageous for lowering human

dose requirements. Furthermore, compound **5** demonstrated both a reasonable bioavailability and half-life for further *in vivo* testing.

Table 2. *in vitro* ADME and *in vivo* PK parameters of **5**

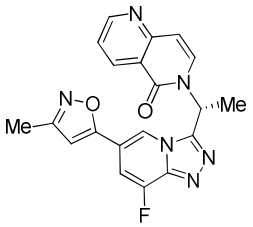

Compound	**5**
RLM Cl[a] (μL/min/mg)	8
MLM Cl[a] (μL/min/mg)	<5
HLM Cl[a] (μL/min/mg)	14
Plasma f_u[b] rat	0.196
mouse	0.245
human	0.320
Rat pharmacokinetics[c]	
Cl (L/h/kg)[d]	0.38
Cl_u (L/h/kg)	1.9
V_{ss} (L/kg)	0.4
$T_{1/2}$ (h)	0.8
F (%)[e]	44

[a]In vitro (RLM = rat liver microsomes; MLM = mouse liver microsomes; HLM = human liver microsomes). [b]Plasma unbound fraction (f_u) was measured using equilibrium dialysis; concentration = 5 μg/mL. [c]*In vivo* experiments were carried out using male Sprague-Dawley rats n = 3. [d]*iv*, 0.25 mg/kg (DMSO). [e]*po*, 2 mg/kg (2% hydroxypropyl methylcellulose 1% Tween 80 in water, pH 2.2).

To demonstrate efficacy and target coverage over time of compound **5** *in vivo*, a PD assay measuring changes in HGF-induced phosphorylation of MET in mouse liver was used (Figure 4). Mice

were administered a single dose of **5** at 10 mg/kg by oral gavage. Human recombinant HGF was injected intravenously at 1, 3, 6, 9, 12 or 24 hours post-dose. Liver and blood were harvested 5 minutes after administration of recombinant HGF. MET phosphorylation was inhibited at least 91% for 9 hours with an associated unbound plasma concentration of 193 nM, covering both the cellular IC_{50} and IC_{90}.

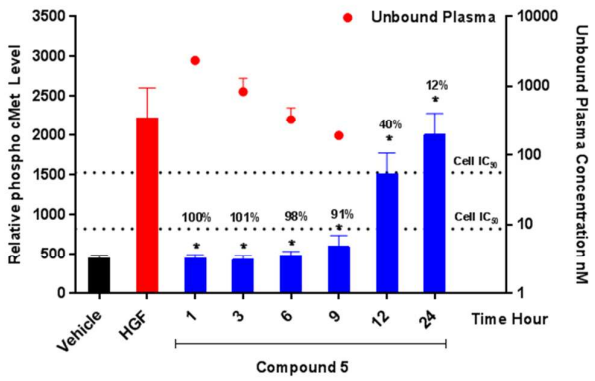

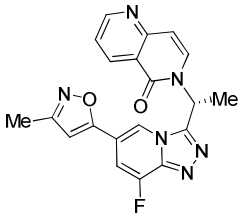

5

Figure 4. Compound **5** inhibited HGF-induced phosphorylation of MET over time in the mouse liver PD assay after oral administration at 10 mg/kg (10 mL/kg dose volume, formulated in 2% hydroxypropyl methylcellulose 1% Tween 80 in water, pH 2.2 adjusted with methanesulfonic acid). Data represent the mean +/- standard deviation (n = 3 mice per group). Statistical significance was determined by ANOVA followed by Bonferroni/Dunn post hoc test. * = $p<0.0001$ compared to HGF control. Red circles represent the mean terminal unbound concentration of **5** in the plasma +/- standard deviation (n = 3 mice per group).

On the basis of the desirable solubility, lack of TDI and robust *in vivo* efficacy of compound **5** in our PD models, we sought a general synthetic method to allow for rapid preparation of naphthyridinone analogs substituted at the C-3 position; substitution at this position had proved pivotal for improving physicochemical properties, metabolism and potency in previous series (e.g. compounds **3** and **4**). In addition, variation at the C-6' position was also important, since both the 3-methyl-isoxazole and the *N*-methyl pyrazole were good partners with the triazolopyridine core (e.g. compound **4**). Finally, since fluorine at the 8-position was not always necessary in previous series, variation of this substituent was also included in the SAR.

The synthesis of compound **5** analogs began with a Suzuki reaction between 5-chloro-2,3-difluoropyridine (**6a**) or 5-bromo-2-fluoropyridine (**6b**) and (3-methylisoxazol-5-yl)boronic acid or a Stille reaction with 1-methyl-4-(tributylstannyl)-1*H*-pyrazole, yielding fluoropyridine intermediates **8b-d** (Scheme 3). **8b-d** were combined with hydrazine in *i*-PrOH and warmed to afford hydrazines **9b-d**. Naphthyridinones substituted at the C-3 position were derived through an annulation reaction between commercially available ethyl 5-bromo-2-methylnicotinate (**16**) and 1,3,5-triazine under basic conditions producing 3-bromo-1,6-naphthyridin-5(6*H*)-one (**17**) in 91% yield.[23] Substitution of bromine was achieved by heating with NaOMe/MeOH or $MeOCH_2CH_2ONa/MeOCH_2CH_2OH$ in the presence of 3,4,7,8-tetramethyl-1,10-phenanthroline and CuI as catalysts to provide naphthyridinones intermediates **10b**,**c**. Exposure of **10b**,**c** and (±)-ethyl 2-iodopropanoate to Cs_2CO_3 in THF at elevated temperature generated racemic ethyl esters **12b**,**c**, which were converted to the corresponding carboxylic acids **13b**,**c** through treatment with an aqueous solution of HCl. HATU mediated coupling of the **13b-c** with hydrazines **9a-d** yielded the hydrazide intermediates, which underwent dehydration with DEAD, $TMSN_3$ and PPh_3 to give triazolopyridines **5**, **18-25** after chiral separation.[24]

Scheme 3. Synthesis of naphthyridinones (**5**, **18-25**)

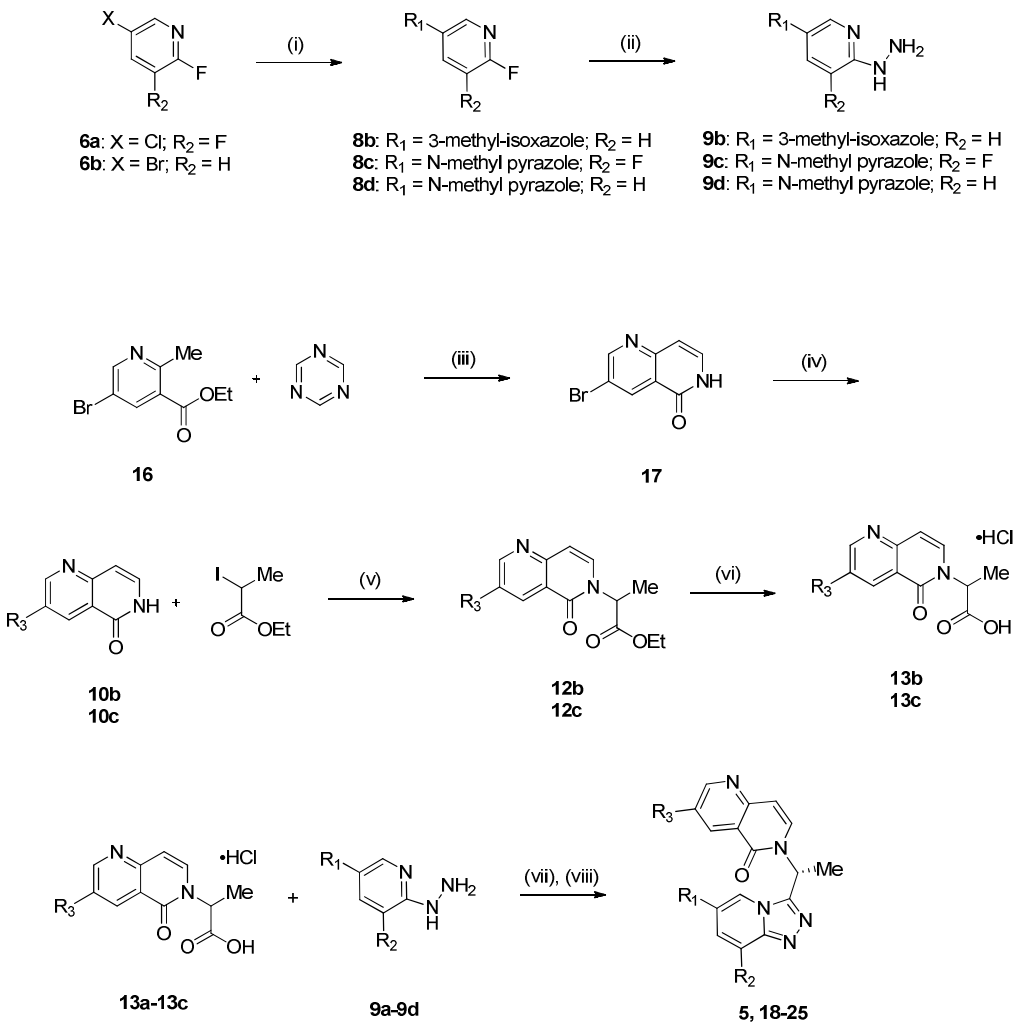

[a]Reagents and conditions: (i) for **8b**: 3-methyl-5-(tributylstannyl)isoxazole, $Pd_2(dba)_3$, $P(t\text{-}Bu)_3{\bullet}BF_4$, CsF, 1,4-dioxane, 90 °C, 12 h, 66%; for **8c**: 1-methyl-4-(4,4,5,5-tetramethyl-1,3,2-dioxaborolan-2-yl)-1*H*-pyrazole, $Pd(OAc)_2$, X-Phos, K_3PO_4, 1,4-dioxane/water, 100 °C, 45 min, 81%; for **8d**: 1-methyl-4-(4,4,5,5-tetramethyl-1,3,2-dioxaborolan-2-yl)-1*H*-pyrazole, $PdCl_2$(dppf), Cs_2CO_3, 1,4-dioxane/water, 90 °C, 3 h, 87%; (ii) NH_2NH_2, *i*-PrOH, for **9b**: 60 °C, 2 h, 96%; for **9c**: 65 °C, 3 h, 97%; for **9b**: 60 °C, 48 h, 98%; (iii) *t*-BuOK, DMSO, 80 °C, 1 h, 91%; (iv) 3,4,7,8-tetramethyl-1,10-phenanthroline, CuI, for **10b**: MeONa, MeOH, 130 °C, 24 h, 89% (75% pure); for **10c**: *t*-BuONa, $MeOCH_2CH_2OH$, 124 °C, 21 h, 85% (v) Cs_2CO_3, THF, for **12b**: DMF, 70 °C, 18 h, 40%; **12c**: THF, 60 °C, 90 min, 53%; (vi) aq. HCl, for **13b**: 80 °C, 10 h, 85%; for **13c**: THF, 65 °C, 4 h, 78%; (vii) for HATU, Hunig's base, MeCN or DMF, 23 °C, 1-3 h, 23-92%; (viii) PPh_3, $TMSN_3$, DEAD, THF, 23 °C, 1-3 h, 20-73%; then chiral separation.

Table 3. Representative naphthyridinones

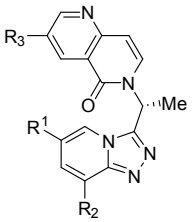

Compound	R^1	R^2	R^3	Biochemical IC_{50} (nM)[a]	Cellular IC_{50}(nM)[b]	LipE[c]	cLogP
5	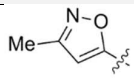	F	H	3	9	7.3	1.2
18		F	MeO	2	5	7.2	1.6
19		F	$MeOCH_2CH_2O$	1	7	7.5	1.5
20		H	$MeOCH_2CH_2O$	2	7	7.4	1.3
21	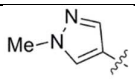	F	H	2	8	7.8	0.9
22		F	MeO	1	6	7.6	1.3
23		F	$MeOCH_2CH_2O$	1	5	7.9	1.1
24		H	MeO	9	11	7.0	1.1
25		H	$MeOCH_2CH_2O$	3	8	7.5	1.0

[a]Inhibition of MET kinase activity, $n \geq 2$. [b]Inhibition of HGF-mediated MET phosphorylation in PC3 cells, $n \geq 2$. [c]LipE = pIC_{50} - clog P.

Consistent with SAR completed in the series involving compounds **3** and **4**, enzyme and cellular potencies were maintained across multiple variations made within the naphthyridinone series with LipE ranging from 7.0 to 7.9 (Table 3). C-6' substitution with methylisoxazoles (*eg.* **5**, **18-20**) and methylpyrazoles (e.g. **21-25**) appeared interchangeable with respect to potency. The addition of methoxy (**18**, **22**, **24**) or methoxyethoxy (**19**, **20, 23, 25**) groups at the C-3 position of the naphthyridinone, installed for the purposes of improving solubility, were also well tolerated and maintained or slightly increased the enzymatic potency (2-3x) when compared to the unsubstituted naphthyridinones **5** or **21**. Finally, replacement of fluorine with hydrogen only had an impact on potency in the pyrazole analogs (**22** *vs* **24** and **23** *vs* **25**), showing a slight decrease in enzyme potency (4-6x).

Table 4. *in vitro* ADME and *in vivo* PK parameters of naphthyridinones **5, 18-25**

Compound	**5**	**18**	**19**	**20**	**21**	**22**	**23**	**24**	**25**
RLM Cl[a] (μL/min/mg)	8	--	16	9	8	12	6	9	<5
MLM Cl[a] (μL/min/mg)	<5	--	14	23	<5	7	8	7	7
HLM Cl[a] (μL/min/mg)	14	--	20	7	<5	<5	9	<5	8
Plasma f_u[b] rat	0.196	--	0.080	0.190	0.271	0.139	0.174	0.206	0.296
mouse	0.245	--	0.317	0.435	0.376	0.353	0.366	0.409	0.424
human	0.320	--	0.409	0.338	0.478	0.309	0.419	0.286	0.498
Rat pharmacokinetics[c]									
Cl (L/h/kg)[d]	0.38	0.46	0.20	0.29	0.28	0.12	0.27	0.65	0.70
Cl_u (L/h/kg)	1.9	--	2.4	1.5	1.0	0.9	1.6	3.2	2.4
V_{ss} (L/kg)	0.4	0.5	0.7	1.0	0.7	0.5	0.9	1.2	1.3
$T_{1/2}$ (h)	0.8	1.1	2.9	2.4	4.0	3.6	3.0	1.7	1.8
F (%)[e]	44	31	54	59	31	43	30	36	25

[a]*In vitro* (RLM = rat liver microsomes; MLM = mouse liver microsomes; HLM = human liver microsomes). [b]Plasma unbound fraction (f_u) were measured using equilibrium dialysis; Concentration = 5 μg/mL. [c]*In vivo* experiments with male Sprague-Dawley rats (n = 3). [d]*iv*, 0.25 mg/kg (DMSO). [e]*po*, 2 mg/kg (2% hydroxypropyl methylcellulose 1% Tween 80 in water, pH 2.2 adjusted with methanesulfonic acid)

The metabolic stability and pharmacokinetic properties of **18-25** were evaluated (Table 4). For all compounds, low microsomal clearance was observed across species. The free fraction in rat, mouse and human plasma were high, consistent with data collected for compound **5**. No obvious differentiation was observed based upon their respective unbound clearances (Cl_u) and oral bioavailabilities (F). Therefore, the *in vivo* half-life was used as the determining factor to prioritize the candidates for additional profiling.

Analogs represented by compound **4**, bearing a $MeOCH_2CH_2O$- solubilizing group demonstrated a consistent cross-species metabolic profile in contrast to their H- or MeO- counterparts.[25] Consistent with

previous observations, when inhibitors **20** and **23** were incubated with NADPH in the presence of liver microsomes, their metabolic profiles were relatively consistent across species, showing demethylation of the $MeOCH_2CH_2O$- side chain and subsequent oxidation to the acid. Consequently, compounds **19**, **20** and **23** were selected for advancement into a PD time-course study with the expectation that their longer half-lives would translate into extended duration of coverage.

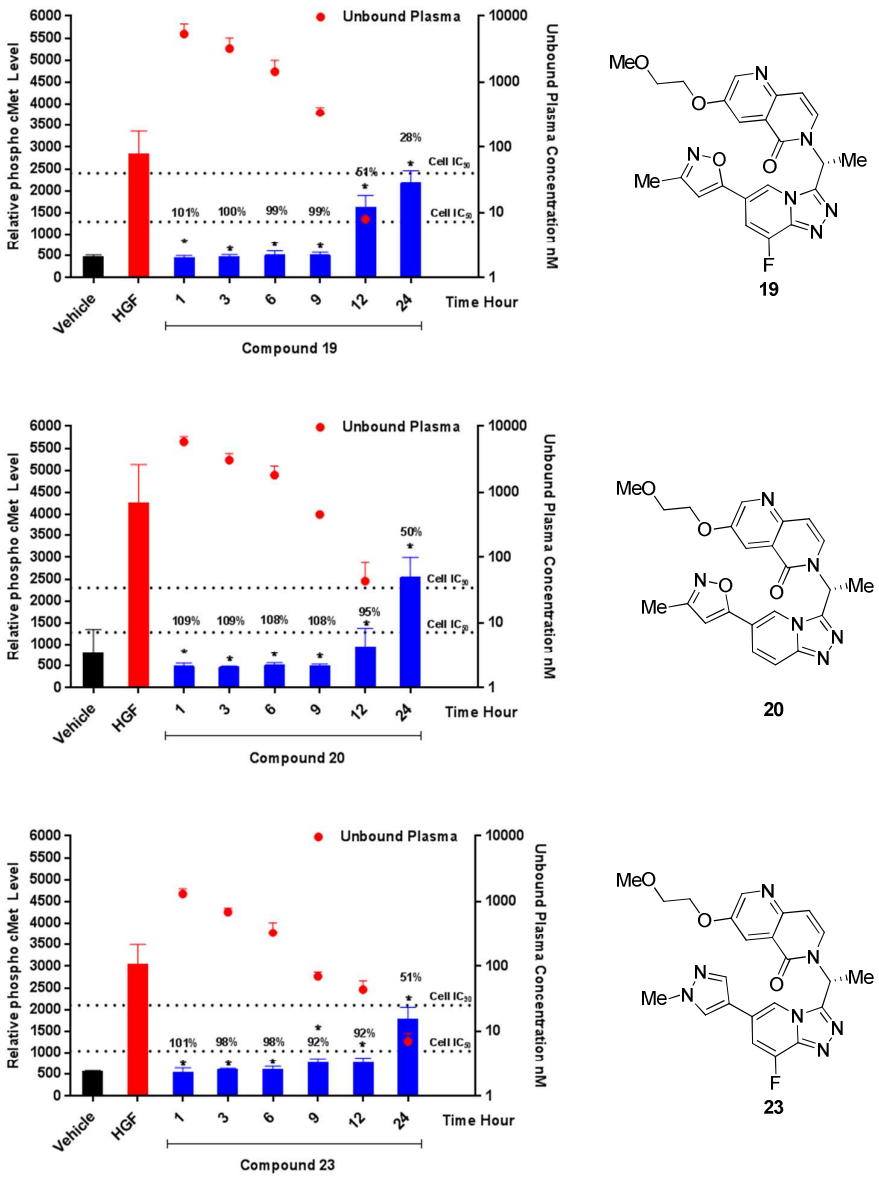

Figure 5. The effect of **19**, **20** and **23** on HGF-induced phosphorylation of MET over time in the mouse liver PD assay after oral administration at 10 mg/kg (10 mL/kg dose volume, formulated in 2% hydroxypropyl methylcellulose 1% Tween 80 in water, pH 2.2 adjusted with methanesulfonic acid). Data represent the mean +/- standard deviation (n = 3 mice per group). Statistical significance was determined by

ANOVA followed by Bonferroni/Dunn post hoc test. * = p<0.0001 compared to HGF control. Red circles represent the mean terminal unbound concentration of compound **19**, **20** or **23** in the plasma +/- standard deviation (n = 3 mice per group).

When dosed at 10 mg/kg, unlike compounds **5** and **19**, compounds **20** and **23** exhibited extended inhibition of MET activity in mice, achieving >90% inhibition of HGF-induced phosphorylation of MET for at least 12 hours (Figure 5). Furthermore, compounds **20** and **23** maintained approximately 50% inhibition over a 24 hour period. Based on these results, **20** and **23** were selected as structurally diverse candidates for PK profiling in a second preclinical species.

Table 5. Dog PK parameters of **20** and **23**

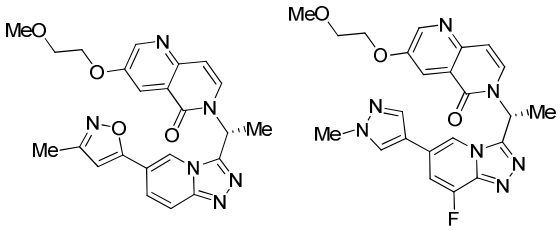

Compound	**20**	**23**
Dog pharmacokinetics[a]		
Cl (L/h/kg)	0.30[b]	0.23[c]
Cl_u (L/h/kg)[d]	0.68	0.46
V_{ss} (L/kg)	1.4	1.1
$T_{1/2}$ (h)	4.3	5.9
10 mg/kg $AUC_{0\rightarrow\infty}$ (μg*h/L)	19300	21000
F (%)	53[e]	49[f]
30 mg/kg $AUC_{0\rightarrow\infty}$ (μg*h/L)	94100	82600
F (%)	87[e]	64[f]

[a]*In vivo* experiments with male beagle dogs (n = 3). [b]*iv* 0.425 mg/kg (20% hydroxypropyl beta-cyclodextrin in water). [c]*iv* 0.713 mg/kg (20% hydroxypropyl beta-cyclodextrin in water, pH 3.5 adjusted with methanesulfonic acid). [d]Unbound fraction (f_u) were measured using equilibrium dialysis; Concentration = 5 µg/mL. [e]*po* (2% hydroxypropyl methylcellulose 1% Tween 80 in water, pH 2.0 adjusted with methanesulfonic acid). [f]*po* (2% hydroxypropyl methylcellulose 1% Tween 80 in water, pH 2.2 adjusted with methanesulfonic acid).

Compounds **20** and **23** showed low clearance (0.30 and 0.23 (L/h/kg)) and moderate volumes of distribution (1.4 and 1.1 L/kg) respectively, with comparable half-lives (4.3 and 5.9 h) following IV administration to beagle dogs (Table 5). After oral dosing at 10 and 30 mg/kg, the AUCs increased proportionally. The bioavailability for **20** was 53% at 10 mg/kg and 87% at 30 mg/kg in comparison to 49% and 64% for compound **23** at the same doses. Overall, both compounds had reasonable dog *iv* and *po* PK properties.

Ultimately, **23** was advanced and evaluated in a MET-dependent xenograft model (Figure 6). Specifically, the NIH-3T3/TPR-Met model derived from NIH3T3 cells transfected with human TPR-Met, an oncogenic form of MET, was employed in this study.[26] Following oral administration (*q.d.*) of **23** at 0.1, 0.3, 1, 3 and 10 mg/kg over 22 days, dose-dependent tumor growth inhibition was observed with an ED_{50} of 0.3 mg/kg and an ED_{90} of 0.8 mg/kg with no adverse effect on body weight.

Tumor Growth Plasma Concentration

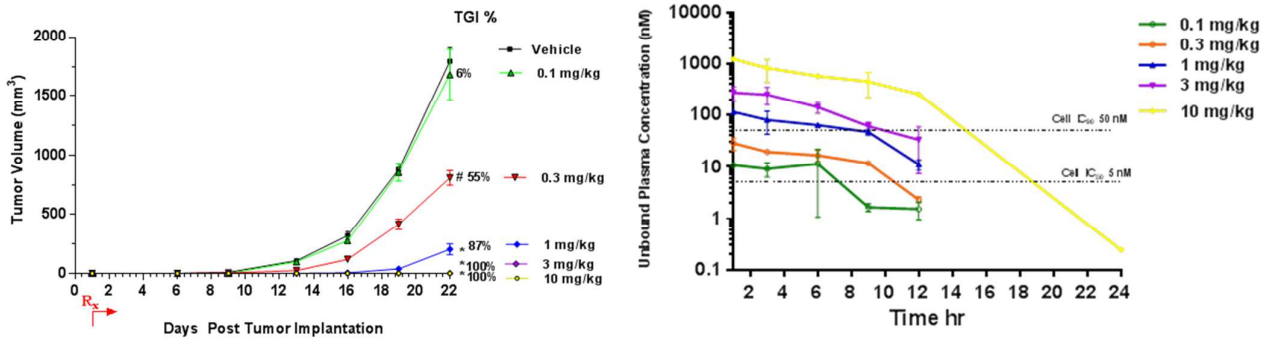

Figure 6. Effect of compound **23** on tumor growth in the NIH-3T3/TPR-Met xenograft model. Compound **23** was administered by oral gavage once per day beginning 24 hours post tumor cell implantation (10 mL/kg dose volume, formulated in 20% hydroxypropyl beta-cyclodextrin in water, pH 3.5 adjusted with methanesulfonic acid). Results are expressed as mean ± standard error (n = 12 per group). Asterisk denotes

p <0.0005 compared to treatment with vehicle. Vehicle: 20% HPBCD, pH 3.5 adjusted with methanesulfonic acid).

Illustrated by the graph of unbound plasma concentration of **23** over time, doses covering the cellular IC_{90} for at least 12 hours (3 and 10 mg/kg) resulted in >90% tumor growth inhibition. Compound **23** did not suffer from TDI of CYP3A4 (IC_{50} >50 μM, IC_{50} w/ preincubation >50 μM), exhibited good solubility in its hydrate form (0.01 N HCl / PBS / SIF (μg/mL): 174 / 77 / >200) and displayed exquisite selectivity against a panel of 402 tyrosine and serine/threonine kinases.[27] These attributes when coupled with its long half-life in rat and dog, its predictable metabolism and good human dose projection convinced us to select compound **23** (AMG 337) as the clinical candidate.

Conclusions

In summary, through rational design guided by our previous work on MET (*eg.* compounds **1-4**), we have generated a new naphthyridinone scaffold that demonstrated nanomolar inhibition of MET kinase activity, improved solubility, a favorable TDI profile and robust *in vivo* efficacy in mouse models of MET-driven tumorigenesis. Moreover, many of the compounds defined by the naphthyridinone scaffold, including **23,** exhibit high LipE and good pharmacokinetics in rat and dog with high unbound concentration in plasma. Compound **23** showed potent and sustained inhibition of MET phosphorylation in a mouse liver pharmacodynamic model and significantly inhibited tumor growth in a MET-dependent mouse efficacy model. **23** is currently in phase two clinical trials.

Experimental Section

Chemistry. Unless otherwise noted, all materials were obtained from commercial suppliers and used as obtained. Anhydrous organic solvents were purchased from Aldrich packaged under N_2 in Sure/Seal™ bottles and used directly. Reactions were monitored using Agilent 1100 Series LCMS with ultraviolet light

(UV) detection at 215 nm and 254 nm and a low resolution electrospray mode (ESI). HRMS data was recorded on Agilent LC-MS TOF (time of flight), Model G1969A instrument. Medium pressure liquid chromatography (MPLC) was performed on a CombiFlash® Companion® (Teledyne Isco) with Redisep® normal-phase silica gel (35-60 micron) columns and UV detection at 254 nm. Purity was measured using Agilent 1100 Series high performance liquid chromatography (HPLC) with UV detection at 215, 254 and 280 nm (15 min; 1.5 mL/min flow rate; eluting with a binary solvent system A and B using a gradient elution (A: water with 0.1% TFA; B: MeCN with 0.1% TFA). Unless otherwise noted, the purity of all compounds was ≥ 95%. Compounds bearing a stereogenic center were purified by preparative supercritical fluid chromatography (SFC) or preparative HPLC using a chiral column. Enantiomeric excess for compounds bearing a stereogenic center were determined using analytical HPLC. ^{1}H NMR spectra were recorded on a Bruker AV-400 (400 MHz) spectrometer at ambient temperature. Chemical shifts are reported in parts per million (δ), and are calibrated using residual undeuterated solvent as an internal reference. Data for ^{1}H NMR spectra are reported as follows: chemical shift (δ ppm) (multiplicity, coupling constant (Hz), integration). Multiplicities are reported as follows: s = singlet, d = doublet, t = triplet, q = quartet, m = multiplet, br = broad, or combinations thereof. Differential scanning calorimetry (DSC) was performed on a TA Instruments Q100 calorimeter at in an aluminum Tzero pan under dry N_2, flowing at 50 mL/min.

Preparation of (*R*)-6-(1-(8-Fluoro-6-(3-methylisoxazol-5-yl)-[1,2,4]triazolo[4,3-*a*]pyridin-3-yl)ethyl)-1,6-naphthyridin-5(6*H*)-one (5) (racemic route):

5-(5,6-Difluoropyridin-3-yl)-3-methylisoxazole (8a): A pressure vessel was charged with 5-chloro-2,3-difluoropyridine (**6a**) (5.00 g, 33.4 mmol), 3-methyl-5-(tributylstannyl)isoxazole (**7**) (18.7 g, 50.2 mmol), XPhos (2.23 g, 4.68 mmol), $PdOAc_2$ (0.53 g, 2.34 mmol) and 1,4-dioxane (170 mL). The vessel was then purged with Ar, sealed and heated at 100 °C for 16 h. After cooling to room temperature, the mixture was concentrated under reduced pressure and purified by MPLC eluting with a gradient of 10-30% EtOAc in hexanes. The resulting solid was triturated with hexanes and filtered to afford 5-(5,6-difluoropyridin-3-yl)-3-methylisoxazole (**8a**) (3.91 g, 60% yield) as a yellow amorphous solid. ^{1}H NMR (400 MHz, DMSO-d_6) δ ppm 8.52 - 8.59 (m, 2 H) 7.07 (s, 1H) 2.31 (m, 3H). LRMS (ESI): m/z (M + H) calcd 197.1; found 197.0.

5-(5-Fluoro-6-hydrazinylpyridin-3-yl)-3-methylisoxazole (9a): A pressure vessel was charged with 5-(5,6-difluoropyridin-3-yl)-3-methylisoxazole (**8a**) (3.68 g, 18.8 mmol), NH_2NH_2 (3.53 mL, 113 mmol) and *i*-PrOH (95.0 mL). The vessel was sealed and warmed to 65 °C for 3 h. Upon cooling to room temperature, the desired product precipitated out of solution. The solid was filtered and washed with *i*-PrOH (2 × 20 mL). The solid was triturated with a saturated solution of $NaHCO_3$ (50 mL), filtered and washed with water (50 mL) to afford 5-(5-fluoro-6-hydrazinylpyridin-3-yl)-3-methylisoxazole (**9a**) (3.46 g, 90% yield) as a white amorphous solid. ^{1}H NMR (400 MHz, DMSO-d_6) δ ppm 8.42 - 8.44 (m, 1 H) 8.37 - 8.38 (m, 1 H) 7.76 (dd, *J*=12.23, 1.86 Hz, 1 H) 6.70 (s, 1 H) 4.33 (br. s., 2 H) 2.25 (s, 3 H). LRMS (ESI): m/z (M + H) calcd 209.1; found 209.2.

(±)-Ethyl 2-(5-oxo-1,6-naphthyridin-6(5*H*)-yl)propanoate (12a): A pressure vessel was charged with 1,6-naphthyridin-5(6*H*)-one (**10a**) (3.00 g, 21.0 mmol), Cs_2CO_3 (13.0 g, 41.0 mmol), ethyl 2-bromopropanoate (**11**) (5.30 mL, 41.0 mmol) and THF (70.0 mL). The vessel was sealed and heated at 60 °C for 3 h. Upon cooling to room temperature, the reaction was diluted with water (200 mL) and extracted with ethyl acetate (2 × 200 mL). The organic phase was dried over anhydrous Na_2SO_4, filtered and concentrated under reduced pressure. The residue was purified by MPLC eluting with a gradient of 0-5% DCM:MeOH (90:10) in DCM to afford (±)-Ethyl 2-(5-oxo-1,6-naphthyridin-6(5*H*)-yl)propanoate (**12a**) (5.29 g, quantitative) as a yellow oil. ^{1}H NMR (400 MHz, DMSO-d_6) δ ppm 8.94 (dd, *J*=4.55, 1.81 Hz, 1 H) 8.52 (ddd, *J*=8.09, 1.83, 0.73 Hz, 1H) 7.76 (d, *J*=7.73 Hz, 1H) 7.53 (dd, *J*=8.07, 4.55 Hz, 1H) 6.76 (dd, *J*=7.63, 0.68 Hz, 1H) 5.32 (q, *J*=7.17 Hz, 1H) 4.13 (q, *J*=7.14 Hz, 2H) 1.62 (d, *J*=7.24 Hz, 3H) 1.15 (t, *J*=7.09 Hz, 3H). LRMS (ESI): m/z (M + H) calcd 247.1; found 247.2.

(±)-2-(5-Oxo-1,6-naphthyridin-6(5*H*)-yl)propanoic acid hydrochloride (13a): A round-bottom flask equipped with a reflux condenser was charged with ethyl (±)-ethyl 2-(5-oxo-1,6-naphthyridin-6(5*H*)-yl)propanoate (**12a**) (5.29 g, 21.5 mmol) and a 6N HCl solution (10.0 mL, 330 mmol). The reaction was heated at 60 °C for 7 h. Additional conc. HCl (~5 mL) was added over the course of the 7 h until complete

hydrolysis was observed. The reaction mixture was cooled to room temperature and concentrated under reduced pressure to afford (±)-2-(5-oxo-1,6-naphthyridin-6(5*H*)-yl)propanoic acid hydrochloride (**13a**) as a dark yellow amorphous solid which was used without further purification. ^{1}H NMR (400 MHz, DMSO-d_6) δ 12.92 (br. s., 2H), 9.07 (dd, *J*=1.76, 5.09 Hz, 1H), 8.81 (ddd, *J*=0.60, 1.80, 7.80 Hz, 1H), 7.97 (d, *J*=7.73 Hz, 1H), 7.74 (dd, *J*=5.04, 8.07 Hz, 1H), 6.91 (dd, *J*=0.59, 7.73 Hz, 1H), 5.35 (q, *J*=7.20 Hz, 1H), 1.62 (d, *J*=7.34 Hz, 3H) LRMS (ESI): m/z (M + H) calcd 219.1; found 219.2.

(*R*)-6-(1-(8-Fluoro-6-(3-methylisoxazol-5-yl)-[1,2,4]triazolo[4,3-*a*]pyridin-3-yl)ethyl)-1,6-naphthyridin-5(6*H*)-one (5): A round-bottom flask was charged with (±)-2-(5-oxo-1,6-naphthyridin-6(5*H*)-yl)propanoic acid hydrochloride (**13a**) (151 mg, 593 μmol), 5-(5-fluoro-6-hydrazinylpyridin-3-yl)-3-methylisoxazole (**9a**) (136 mg, 652 μmol), HATU (293 mg, 771 μmol) in DMF (3 mL) under an atmosphere of N_2. The reaction mixture was treated with Hunig's base (311 μL, 1.78 mmol) and stirred at room temperature for 3 h. The reaction mixture was concentrated under reduced pressure and the residue was then quickly passed through a plug of silica gel eluting with a gradient of 0-100% DCM:MeOH:NH_4OH (90:10:10) in DCM, concentrated under reduced pressure and use without further purification.

In a round-bottom flask the product was then suspended in THF (6.00 mL) under an atmosphere of N_2 and treated with PPh_3 (233 mg, 889 μmol) and $TMSN_3$ (118 μL, 889 μmol). DEAD (141 μL, 889 μmol) was introduced and the reaction was allowed to stirred for 3 h. The reaction mixture was passed through a conditioned Isolute ® SPE column (SCX-2) and washed with MeOH (3 × 25 mL). The compound was then released from the column using a solution of ammonia in MeOH (2.0 M, 3 × 25 mL) and the solution was concentrated under reduced pressure. The residue was purified by MPLC eluting with a gradient of 0-100% DCM:MeOH:NH_4OH (90:10:10) in DCM to afford (±)-6-(1-(8-fluoro-6-(3-methylisoxazol-5-yl)-[1,2,4]triazolo[4,3-a]pyridin-3-yl)ethyl)-1,6-naphthyridin-5(6*H*)-one (**5**) (120 mg, 52% yield over two steps) as a white amorphous solid. ^{1}H NMR (400 MHz, DMSO-d_6) δ 8.92 (dd, *J*=1.81, 4.55 Hz, 1H), 8.81 (d, *J*=1.08 Hz, 1H), 8.62 (ddd, *J*=0.73, 1.81, 8.12 Hz, 1H), 7.84 (dd, *J*=1.12, 11.49 Hz, 1H), 7.77 (d, *J*=7.82 Hz, 1H), 7.54 (dd, *J*=4.60, 8.12 Hz, 1H), 7.02 (q, *J*=7.10 Hz, 1H), 7.01 (s, 1H), 6.78 (dd, *J*=0.54, 7.78 Hz,

1H), 2.27-2.34 (m, 3H), 2.00 (d, *J*=7.14 Hz, 3H). HRMS (ESI): m/z (M + H) calcd 391.1313; found 391.1328. The enantiomers of (±)-**5** were seperated by high performance liquid chromatography (HPLC) through repeated 1.5 mL injections of a 14 mg/mL solution onto a Chiralpak IA-H, 3 cm × 25 cm (i.d. × length) column. Isocratic elution with EtOH:Heptane (1:1) at a flowrate of 45 mL/min provided 52 mg of peak 1 (***ent*-5**) (*ee* > 99%) and 53 mg of peak 2 (**5**) (*ee* > 99%).

Alternative preparation of (*R*)-6-(1-(8-Fluoro-6-(3-methylisoxazol-5-yl)-[1,2,4]triazolo[4,3-*a*]pyridin-3-yl)ethyl)-1,6-naphthyridin-5(6*H*)-one (5) (enantioselective route):

(*R*)-2-(5-Oxo-1,6-naphthyridin-6(5*H*)-yl)propanoic acid hydrochloride (15): A round-bottom flask equipped with an addition funnel was charged with 1,6-naphthyridin-5(6*H*)-one (**10a**) (90.8 g, 620 mmol), PPh_3 (260 g, 994 mmol) and (*S*)-(-)-lactic acid methyl ester (**14**) (74.0 mL, 780 mmol) in THF (1.20 L) and the mixture was cooled in an ice bath. To this mixture was added DEAD (150 mL, 930 mmol) drop-wise, while maintaining a reaction temperature below 15 °C Following addition, the reaction temperature was stabilized at 10 °C, the ice bath was removed. An additional portion of THF (200 mL) was introduced and the reaction mixture stirred for an additional 10 h. The reaction mixture was concentrated under reduced pressure and azeotroped with EtOAc (2 × 250 mL). The reaction vessel was equipped with an overhead stirrer and the reaction mixture was partitioned between a 6N HCl solution (1.0 L) and Et_2O (1.5 L). The layers were separated and the organic layer was extract with 6N HCl (2 × 300 mL). The combined aqueous layers were filtered through a fritted filter and transferred to a 3-neck round-bottom flask equipped with a condenser and overhead stirrer. The reaction mixture was heated to 75 °C for 10 h then allowed to cool to room temperature. Additional 6N HCl solution (500 mL) was introduced and the reaction mixture was washed with EtOAc (3 × 500 mL). The aqueous layer was concentrated under reduce pressure to produce a thick slurry (~500 mL). The slurry was cooled 0 °C and the precipitate was filtered and washed with cold MeCN to afford (*R*)-2-(5-oxo-1,6-naphthyridin-6(5*H*)-yl)propanoic acid hydrochloride (**15**) (107 g, 67% yield over two steps) as a light yellow amorphous solid. An analytical sample was confirmed to be >95% *ee*. Analysis performed by HPLC, Chiralpak AD-H, 4.6 x 250 mm, 25% EtOH w/ 0.1% TFA and 75% heptane, flowrate = 1 mL/min, detection = 215 nm.

(*R*)-6-(1-(8-Fluoro-6-(3-methylisoxazol-5-yl)-[1,2,4]triazolo[4,3-*a*]pyridin-3-yl)ethyl)-1,6-naphthyridin-5(6*H*)-one (5): A 250-mL, two-neck, round-bottom flask equipped with a 25-mL addition funnel was charged with a suspension of (*R*)-2-(5-oxo-1,6-naphthyridin-6(5*H*)-yl)propanoic acid hydrochloride (**15**) (4.00 g, 16.0 mmol), 1-(3-fluoro-5-(3-methylisoxazol-5-yl)pyridin-2-yl)hydrazine (**9a**) (3.60 g, 17.0 mmol) and HATU (9.00 g, 24.0 mmol) in MeCN (50 mL) under an atmosphere of N_2. The reaction mixture was cooled to 0 ºC in an ice bath before Hunig's base (8.2 mL, 47 mmol) was added drop-wise to the rapidly stirred suspension over 30 minutes, while maintaining an internal temperature below 10 ºC in order to avoid racemization.[28] Following addition, the reaction was warmed to room temperature over 30 minutes and concentrated under reduced pressure. The residue was then quickly passed through a plug of silica gel and eluted with a gradient of 0-100% DCM:MeOH:NH_4OH (90:10:10) in DCM to afford (*2R)-N′*-(3-fluoro-5-(3-methylisoxazol-5-yl)pyridin-2-yl)-2-(5-oxo-1,6-naphthyridin-6(5*H*)-yl)propanehydrazide which was used without further purification.

In a round-bottom flask, crude (*2R*)-*N′*-(3-fluoro-5-(3-methylisoxazol-5-yl)pyridin-2-yl)-2-(5-oxo-1,6-naphthyridin-6(5*H*)-yl)propanehydrazide (1.90 g, 4.70 mmol) was resuspended in THF (50 mL). PPh_3 (1.80 g, 7.00 mmol) was introduced and the reaction vessel was purged with N_2. The reaction was cooled to 0 ºC and treated with $TMSN_3$ (930 µL, 7.00 mmol) follow by slow addition of DEAD (1.10 mL, 7.00 mmol) via syringe, while maintaining an internal the reaction temperature below 30 ºC. After 1 h, the reaction mixture was concentrated under reduced pressure and partitioned between EtOAc (300 mL) and 2N HCl solution (300 mL). The aqueous layer was collected and the organic layer was extracted with 2N HCl solution (2 × 300 mL). The combined aqueous layers were cooled to 0 ºC and neutralized with an aqueous 6N NaOH solution to pH 7. The precipitate was filtered and washed with cold H_2O (2 × 50.0 mL) and cold EtOH (50.0 mL). The solid was purified by slow recrystallization in EtOH to afford (*R*)-6-(1-(8-fluoro-6-(3-methylisoxazol-5-yl)-[1,2,4]triazolo[4,3-a]pyridin-3-yl)ethyl)-1,6-naphthyridin-5(6*H*)-one (**5**) (1.50 g, 83% yield). An analytical sample was confirmed to be >99% *ee*. Analysis performed by HPLC, Chiralpak AD-H, 4.6 x 100 mm, EtOH:Heptane (1:1), flowrate = 1 mL/min, detection = 215 nm. The isolated solid exists

as crystalline anhydrous free base form II displaying two melts: a melt at 200-239 ºC and final melt at 292-299 ºC. ^{1}H NMR and LRMS data are consistent with compound **5** from the racemic synthesis.

Preparation of 18-25:

5-(6-Fluoropyridin-3-yl)-3-methylisoxazole (8b): A 3-neck round-bottom flask equipped with an overhead stirrer, temperature probe and reflux condenser was charged with 3-methyl-5-(tributylstannyl)isoxazole (233 g, 625 mmol), 5-bromo-2-fluoropyridine (**6b**) (100 g, 568 mmol), (t-Bu)$_3$P•BF$_4$ (16.5 g, 56.8 mmol), Pd$_2$(dba)$_3$ (26.0 g, 28.4 mmol) and 1,4-dioxane (1.25 L). CsF (173 g, 1.14 mol) was slowly added to the stirred reaction mixture. Following addition, the reaction mixture was warmed to 90 °C (internal temperature). After 12 h, the reaction mixture was cooled to room temperature and concentrated under reduced pressure. The crude material was suspended in EtOAc (1.0 L) and filtered through a silica-gel plug. The plug was eluted with EtOAc (~3.0 L) and the filtrate was concentrated under reduced pressure. The resulting solid was triturated with acetonitrile (~200 mL) and allowed to age at 0 °C for 30 minutes. The solid was filtered and washed with cold acetonitrile (25 mL) and hexanes (25 mL). The filtrate was concentrated under reduced pressure and the solid was triturated with Et$_2$O (200 mL). The resultant solid was filtered and washed with Et$_2$O (25 mL) and hexanes (25 mL). The two batches of solid were combined to afford 5-(6-fluoropyridin-3-yl)-3-methylisoxazole (**8b**) (66.4 g, 66 % yield) as a pale yellow amorphous solid. ^{1}H NMR (400 MHz, CHLOROFORM-d) δ 8.64 (d, J=2.45 Hz, 1H), 8.18 (ddd, J=2.49, 7.43, 8.56 Hz, 1H), 7.07 (ddd, J=0.68, 3.01, 8.53 Hz, 1H), 6.44 (s, 1H), 2.40 (s, 3H) LRMS (ESI): m/z (M + H) calcd 179.1; found 179.1.

5-(6-Hydrazinylpyridin-3-yl)-3-methylisoxazole (9b): A 3-neck round-bottom flask equipped with an overhead stirrer, internal temperature probe and reflux condenser was charged with 5-(6-fluoropyridin-3-yl)-3-methylisoxazole (**8b**) (66.4 g, 373 mmol) in i-PrOH (760 mL). To this suspension, hydrazine (70.2 mL, 2.24 mol) was added and the reaction mixture was heated at 60 °C (internal temperature) for 2 h. The reaction mixture was cooled to 0 °C and allowed to age for 1 hour. The precipitate was filtered and washed with cold i-PrOH to afford 5-(6-hydrazinylpyridin-3-yl)-3-methylisoxazole dihydrofluoride (**9b**) (82.6 g, 96

% yield). ^{1}H NMR (400 MHz, DMSO-d_6) δ 8.44 (dd, *J*=0.68, 2.35 Hz, 1H), 8.02 (s, 1H), 7.82 (dd, *J*=2.35, 8.80 Hz, 1H), 6.79 (d, *J*=8.80 Hz, 1H), 6.59 (s, 1H), 4.28 (br. s., 2H), 3.30 (br. s., 1H), 2.24 (s, 3H) LRMS (ESI): m/z (M + H) calcd 191.1; found 191.1.

2,3-Difluoro-5-(1-methyl-1*H*-pyrazol-4-yl)pyridine (8c): A 3-neck flask equipped with an overhead stirrer, internal temperature probe and reflux condenser under an atmosphere of N_2 was charged with $Pd(OAc)_2$ (6.01 g, 26.8 mmol), X-Phos (25.5 g, 53.5 mmol), 1-methyl-4-(4,4,5,5-tetramethyl-1,3,2-dioxaborolan-2-yl)-1*H*-pyrazole (134 g, 642 mmol), and a mixture of 1,4-dioxane (1550 mL) and water (150 mL). To this mixture was added 5-chloro-2,3-difluoropyridine (**6a**) (80.0 g, 535 mmol) and K_3PO_4 (341 g, 1.61 mol). The internal temperature was raised to 97 °C and the reaction mixture was stirred for 45 min. The reaction mixture was allowed to cool to ~80 °C and filtered through a pad of celite which was subsequently washed with EtOAc (500 mL). The organic layer was washed with an aqueous solution of NaCl sat. (250 mL). The organic layer was concentrated under reduced pressure, the residue was triturated with warm Et_2O (500 mL), cooled to room temperature and the solid was filtered and washed with Et_2O (100 mL) to afford 2,3-difluoro-5-(1-methyl-1*H*-pyrazol-4-yl)pyridine (**8c**) (84.9 g, 81% yield) as an off-white amorphous solid. ^{1}H NMR (400 MHz, DMSO-d_6) δ 8.23-8.31 (m, 2H), 8.28 (s, 1H), 7.99 (d, *J*=0.68 Hz, 1H), 3.87 (s, 3H). LRMS (ESI): m/z (M + H) calcd 196.1; found 196.2.

3-Fluoro-2-hydrazinyl-5-(1-methyl-1*H*-pyrazol-4-yl)pyridine (9c): A 3-neck round-bottom flask equipped with an overhead stirrer, internal temperature probe and reflux condenser was charged with 2,3-difluoro-5-(1-methyl-1*H*-pyrazol-4-yl)pyridine (**8c**) (65.4 g, 335 mmol) and NH_2NH_2•H_2O (114 mL, 2.35 mol) in *i*-PrOH (170 mL). The reaction mixture was heated at 65 °C for 3 h and then diluted with *i*-PrOH (75 mL) and cooled in an ice bath. The solid was filtered and triturated with an aqueous solution of saturated $NaHCO_3$ (20 mL), filtered and washed with Et_2O to afford 3-fluoro-2-hydrazinyl-5-(1-methyl-1*H*-pyrazol-4-yl)pyridine (**9c**) (67.2 g, 97% yield) as a white amorphous solid. ^{1}H NMR (400 MHz, DMSO-d_6)

δ 8.16 (t, *J*=1.50 Hz, 1H), 8.05 (d, *J*=0.50 Hz, 1H), 7.80 (d, *J*=0.78 Hz, 1H), 7.68 (s, 1H), 7.59 (dd, *J*=1.86, 12.72 Hz, 1H), 4.12 (s, 2H), 3.84 (s, 3H). LRMS (ESI): m/z (M + H) calcd 208.1; found 208.3.

2-Fluoro-5-(1-methyl-1*H*-pyrazol-4-yl)pyridine (8d): A pressure vessel was charged with $PdCl_2$(dppf)•DCM adduct (3.25 g, 3.98 mmol), Cs_2CO_3 (38.9 g, 119 mmol), 1-methyl-4-(4,4,5,5-tetramethyl-1,3,2-dioxaborolan-2-yl)-1*H*-pyrazole (9.93 g, 47.7 mmol), 5-bromo-2-fluoropyridine (**6b**) (7.00 g, 39.8 mmol) in 1,4-dioxane (100 mL) and water (10 mL). The reaction was purged with an atmosphere of Ar, sealed and stirred at 90 °C for 3 h. The reaction was cooled to room temperature, concentrated under reduced pressure and purified by MPLC eluting with a gradient of 0-10% DCM:MeOH (90:10) in DCM to afford 2-fluoro-5-(1-methyl-1*H*-pyrazol-4-yl)pyridine (**8d**) (6.10 g, 87% yield) as a tan amorphous solid. ^{1}H NMR (400 MHz, DMSO-d_6) δ 8.46 (ddd, *J*=0.68, 1.25, 2.57 Hz, 1H), 8.22 (d, *J*=0.50 Hz, 1H), 8.14 (ddd, *J*=2.45, 7.82, 8.51 Hz, 1H), 7.94 (d, *J*=0.78 Hz, 1H), 7.18 (ddd, *J*=0.64, 2.98, 8.51 Hz, 1H), 3.87 (s, 3H). LRMS (ESI): m/z (M + H) calcd 178.1; found 178.2.

2-Hydrazinyl-5-(1-methyl-1*H*-pyrazol-4-yl)pyridine (9d): A pressure vessel was charged with 2-fluoro-5-(1-methyl-1*H*-pyrazol-4-yl)pyridine (**8d**) (6.13 g, 34.6 mmol), NH_2NH_2 (5.43 mL, 173 mmol) in *i*-PrOH (200 mL) and stirred at 65 °C. Additional hydrazine (5.43 mL, 173 mmol) was added to the reaction mixture every 12 h over 2 days in order to achieve full consumption of the starting material. The reaction was partially concentrated (~50%) and cooled in an ice bath. The resultant solid was filtered and washed with cold *i*-PrOH to afford 2-hydrazinyl-5-(1-methyl-1*H*-pyrazol-4-yl)pyridine (**9d**) (6.40 g, 98% yield) as a gray amorphous solid. ^{1}H NMR (400 MHz, DMSO-d_6) δ 8.22 (dd, *J*=0.68, 2.35 Hz, 1H), 7.97 (s, 1H), 7.72 (d, *J*=0.68 Hz, 1H), 7.63 (dd, *J*=2.35, 8.61 Hz, 1H), 7.31 (s, 1H), 6.71 (dd, *J*=0.73, 8.66 Hz, 1H), 3.74-3.96 (m, 3H), 3.54 (br. s., 2H). LRMS (ESI): m/z (M + H) calcd 190.1; found 190.2.

3-Bromo-1,6-naphthyridin-5(6*H*)-one (17): A 3-neck round-bottom flask equipped with an internal temperature probe and reflux condenser under an atmosphere of N_2 was charged with ethyl 5-bromo-2-

methylnicotinate (**16**) (100 g, 410 mmol), 1,3,5-triazine (37.0 g, 456 mmol) and dry DMSO (100 mL). The solution was stirred at room temperature for 30 min and *t*-BuOK (52.4 g, 467 mmol) was added, followed by dry DMSO (100 mL). A significant exotherm was observed with an internal temperature rising to 84 °C. The reaction stirred for 30 min and the reaction was heated to 80 °C for an additional 30 min. The reaction mixture was then cooled to room temperature and diluted with water (600 mL) where a precipitate formed. AcOH (27.0 mL, 470 mmol) was added and the solution was stirred at room temperature for 30 minutes. The reaction was then degassed (Warning! HCN is generated during this reaction) by sparging the solution with N_2 for 18 h. The exhaust gas was scrubbed by passage through 6N NaOH (500 mL) to remove excess HCN. Following the purge, the resultant solid was collected by filtration and washed with H_2O and then Et_2O. The resultant orange brown solid was triturated in refluxing MeCN (150 mL) for 15 minutes, then cooled to room temperature. The solid was filtered to afford 3-bromo-1,6-naphthyridin-5(6*H*)-one (**17**) (83.9 g, 91% yield) as a tan solid. ^{1}H NMR (400 MHz, DMSO-d_6) δ 11.75 (br. s, 1H), 9.00 (d, *J*=2.45 Hz, 1H), 8.59 (dd, *J*=0.78, 2.45 Hz, 1H), 7.49 (d, *J*=7.34 Hz, 1H), 6.62 (dd, *J*=0.73, 7.38 Hz, 1H). LRMS (ESI): m/z (M + H) calcd 225.0/227.0; found 225.0/227.0.

3-Methoxy-1,6-naphthyridin-5(6*H*)-one (10b): A sealed Parr reactor was charged with NaOMe (120 g, 2.22 mol) and MeOH (400 mL) followed by 3-bromo-1,6-naphthyridin-5(6*H*)-one (**17**) (50.0 g, 220 mmol), 3,4,7,8-tetramethyl-1,10-phenanthroline (10.5 g, 44.0 mmol), and CuI (4.23 g, 22.0 mmol). The reactor was sealed and heated at 130 °C and stirred for 24 h. The reaction was then cooled to room temperature and the pressure was released. The mixture was transferred to a round-bottom flask and cooled to 0 °C and the reaction was neutralized with H_2O (500 mL) and aqueous 6N HCl solution to pH 7. The solution was diluted with H_2O (500 mL) and extracted with EtOAc (3 × 1.0 L). The organic layer was concentrated under pressure and the solid was dissolved in EtOAc:MeOH (5:1, 1.5 L) and the insoluble brown solid was removed by filtration. The organic layer was washed with an aqueous solution n-(2-hydroxyethyl)ethylenediaminetriacetic acid trisodium salt hydrate (10 wt%, 500 mL). The aqueous phase was separated and extracted with EtOAc (2 × 500 mL), the organic layers were combined and concentrated under reduced pressure to afford 3-methoxy-1,6-naphthyridin-5(6*H*)-one (**10b**) (35.0 g, 89% yield) as a

yellow amorphous solid contaminated with 3,4,7,8-tetramethyl-1,10-phenanthroline (25 wt%). ^{1}H NMR (400 MHz, METHANOL-d_4) δ 8.63 (d, *J*=3.03 Hz, 1H), 8.04 (d, *J*=3.03 Hz, 1H), 7.30 (d, *J*=7.43 Hz, 1H), 6.75 (d, *J*=7.43 Hz, 1H), 3.98 (s, 3H). LRMS (ESI): m/z (M + H) calcd 177.1; found 177.0.

3-(2-Methoxyethoxy)-1,6-naphthyridin-5(6*H*)-one (10c): A 3-neck round-bottom flask equipped with overhead stirrer, temperature probe and reflux condenser under an atmosphere of N_2 was charged with 2-methoxyethanol (1.00 L, 12.7 mol) followed by portion-wise addition of *t*-BuONa (247 g, 2.57 mol) (temperature increased to ~70°C). Following addition, the reaction mixture stirred for an additional 15 minutes. The condenser was removed and the vessel fitted with a short-path distillation apparatus. The temperature was raised to 130 °C and ~140 g of distillate was collected (mostly *t*-BuOH). The reaction was then refitted with a reflux condenser and cooled to 50 °C. 3-Bromo-1,6-naphthyridin-5(6*H*)-one (**17**) (100 g, 444 mmol), 3,4,7,8-tetramethyl-1,10-phenanthroline (23.0 g, 97.0 mmol) and CuI (8.46 g, 44.4 mmol) where introduced and the reaction temperature was raised to 125 °C (internal temperature) for 24 h. The reaction was cooled to room temperature, neutralized with AcOH (153 mL), diluted with EtOAc (2.5 L), stirred briefly. The solution was filtered through a plug of silica gel, which was eluted with 5% MeOH in DCM (5 L). The filtrate was concentrated under reduced pressure, azeotroped with PhMe and the product recrystalized from *i*-PrOH to afford 3-(2-methoxyethoxy)-1,6-naphthyridin-5(6*H*)-one (**10c**) (83.4 g, 85% yield) as a yellow amorphous solid contaminated with a copper impurity (broad NMR). An analytical sample was purified by MPLC eluting with a gradient of 0-100% DCM:MeOH (90:10) in DCM. ^{1}H NMR (400 MHz, DMSO-d_6) δ 11.46 (br. s, 1H), 8.67 (d, *J*=3.03 Hz, 1H), 7.90 (d, *J*=2.84 Hz, 1H), 7.29 (d, *J*=7.63 Hz, 1H), 6.60 (d, *J*=7.34 Hz, 1H), 4.25-4.32 (m, 2H), 3.69-3.74 (m, 2H), 3.32 (s, 3H). LRMS (ESI): m/z (M + H) calcd 121.1; found 221.2.

(±)-**Ethyl 2-(3-methoxy-5-oxo-1,6-naphthyridin-6(5*H*)-yl)propanoate** (**12b**): A round-bottom flask under an atmosphere of N_2 was charged with 3-methoxy-1,6-naphthyridin-5(6*H*)-one (**10b**) (7.61 g, 43.2 mmol), Cs_2CO_3 (6.9 mL, 86 mmol) and THF (100 mL) followed by addition of ethyl 2-bromopropionate

(9.0 mL, 69 mmol) in DMF (50 mL) and heated at 70 °C for 18 h. The reaction was cooled to room temperature and concentrated under reduced pressure. The residue was diluted with water and extracted with EtOAc (3X). The organic layer was dried over $MgSO_4$, filtered and concentrated under reduced pressure. The crude mixture was purified by MPLC eluting with 50% EtOAc in hexanes to afford (±)-ethyl 2-(3-methoxy-5-oxo-1,6-naphthyridin-6(5*H*)-yl)propanoate (**12b**) (3.0 g, 40% yield) as an off-white amorphous solid. ^{1}H NMR (400 MHz, DMSO-d_6) δ 8.70 (d, *J*=3.13 Hz, 1H), 7.90 (dd, *J*=0.59, 3.03 Hz, 1H), 7.61 (d, *J*=7.73 Hz, 1H), 6.74 (dd, *J*=0.64, 7.68 Hz, 1H), 5.30 (q, *J*=7.14 Hz, 1H), 4.12 (q, *J*=7.11 Hz, 2H), 3.93 (s, 3H), 1.61 (d, *J*=7.14 Hz, 3H), 1.15 (t, *J*=7.00 Hz, 3H). LRMS (ESI): m/z (M + H) calcd 277.1; found 277.2.

(±)-**Ethyl 2-(3-(2-methoxyethoxy)-5-oxo-1,6-naphthyridin-6(5*H*)-yl)propanoate (12c)**: A 3-neck round-bottom flask was equipped with a internal temperature probe, overhead stirrer, and reflux condenser under an atmosphere of N_2, then charged with 3-(2-methoxyethoxy)-1,6-naphthyridin-5(6*H*)-one (**10c**) (59.5 g, 270 mmol), Cs_2CO_3 (176 g, 540 mmol) and THF (600 mL). Ethyl 2-bromopropanoate (56.3 mL, 432 mmol) was added to the suspension and the mixture was heated to 60 °C (internal temperature) for 90 minutes. The reaction was cooled to room temperature and filtered through a plug of silica gel eluting with EtOAc and the filtrate was concentrated under reduced pressure. The crude material was purified by MPLC eluting with a gradient of 50-100% EtOAc in DCM to afford (±)-ethyl 2-(3-(2-methoxyethoxy)-5-oxo-1,6-naphthyridin-6(5*H*)-yl)propanoate (**12c**) (45.5 g, 53% yield) as yellow oil. ^{1}H NMR (400 MHz, DMSO-d_6) δ 8.70 (d, *J*=3.03 Hz, 1H), 7.92 (d, *J*=2.84 Hz, 1H), 7.61 (d, *J*=7.73 Hz, 1H), 6.73 (d, *J*=8.02 Hz, 1H), 5.31 (q, *J*=7.14 Hz, 1H), 4.25-4.33 (m, 2H), 4.12 (q, *J*=7.11 Hz, 2H), 3.65-3.78 (m, 2H), 3.32 (s, 3H), 1.61 (d, *J*=7.24 Hz, 3H), 1.15 (t, *J*=7.09 Hz, 3H). LRMS (ESI): m/z (M + H) calcd 321.1; found 321.0.

(±)-**2-(3-Methoxy-5-oxo-1,6-naphthyridin-6(5*H*)-yl)propanoic acid hydrochloride (13b)**: A pressure vessel was charged with ethyl (±)-2-(3-methoxy-5-oxo-1,6-naphthyridin-6(5*H*)-yl)propanoate (**12b**) (3.30 g, 11.9 mmol) in aqueous 6N HCl solution (39.8 mL, 239 mmol) and stirred overnight at 80 °C. The reaction was concentrated under reduced pressure to afford **(±)-**2-(3-methoxy-5-oxo-1,6-naphthyridin-

6(5*H*)-yl)propanoic acid hydrochloride (**13b**) (2.53 g, 85% yield) as a yellow amorphous solid. ^{1}H NMR (400 MHz, DMSO-d_6) δ 8.72 (d, *J*=3.03 Hz, 1H), 7.94 (dd, *J*=0.54, 3.08 Hz, 1H), 7.63 (d, *J*=7.73 Hz, 1H), 6.74 (dd, *J*=0.59, 7.63 Hz, 1H), 5.30 (q, *J*=7.30 Hz, 1H), 4.90 (br. s., 2H), 3.94 (s, 3H), 1.60 (d, *J*=7.24 Hz, 3H). LRMS (ESI): m/z (M + H) calcd 249.1; found 249.2.

(±)-2-(3-(2-Methoxyethoxy)-5-oxo-1,6-naphthyridin-6(5*H*)-yl)propanoic acid hydrochloride (13c): A round-bottom flask equipped with a reflux condenser was charged with (±)-ethyl 2-(3-(2-methoxyethoxy)-5-oxo-1,6-naphthyridin-6(5*H*)-yl)propanoate (**12c**) (45.5 g, 142 mmol) in THF (240 mL) and 6N HCl (240 mL, 1.42 mol). The reaction was stirred at 70 °C for 4 h. The reaction was cooled to room temperature and concentrated under reduced pressure. The solid was triturated with MeCN and cooled to 0 °C and the solid was filtered. The filtrate was concentrated, triturated with MeCN and cooled to 0 °C and also filtered. The two batchs of solid were combined to afford (±)-2-(3-(2-methoxyethoxy)-5-oxo-1,6-naphthyridin-6(5*H*)-yl)propanoic acid hydrochloride (**13c**) (36.6 g, 78% yield) as a yellow amorphous solid. ^{1}H NMR (400 MHz, DMSO-d_6) δ 8.71 (d, *J*=3.03 Hz, 1H), 7.94 (dd, *J*=0.59, 3.03 Hz, 1H), 7.61 (d, *J*=7.73 Hz, 1H), 6.72 (dd, *J*=0.54, 7.68 Hz, 1H), 5.31 (q, *J*=7.34 Hz, 1H), 4.27-4.31 (m, 2H), 3.70-3.74 (m, 2H), 3.32 (s, 3H), 1.60 (d, *J*=7.24 Hz, 3H). LRMS (ESI): m/z (M + H) calcd 293.1; found 293.0.

The following compounds (**18**-**25**) were prepared in a similar fashion as compound **5**.

(*R*)-6-(1-(8-Fluoro-6-(3-methylisoxazol-5-yl)-[1,2,4]triazolo[4,3-*a*]pyridin-3-yl)ethyl)-3-methoxy-1,6-naphthyridin-5(6*H*)-one (18): Step 1: Coupling **9a** and **13b** in MeCN, 1 h, room temperature, 92% yield. LRMS (ESI): m/z (M + H) 438.8. Step 2: THF, 1 h, room temperature, 25% yield. The racemate was purified by supercritical fluid chromatography (SFC) by repeated 0.2 mL injections of a 17 mg/mL solution onto a Chiralpak AD-H, 2 cm x 25 cm (i.d. x length) column, eluting with 40% MeOH w/ 0.2% Et_2NH and 60% CO_2 at a flow rate of 70 mL/min to provide 67 mg of peak 1 (***ent*-18**) with *ee* > 99% and 660 mg peak 2 (**18**) with *ee* = 98%.[29] ^{1}H NMR (400 MHz, DMSO-d_6) δ 8.80 (d, *J*=1.08 Hz, 1H), 8.68 (d, *J*=3.03 Hz, 1H), 7.98 (dd, *J*=0.59, 3.03 Hz, 1H), 7.85 (dd, *J*=1.12, 11.49 Hz, 1H), 7.64 (d, *J*=7.73 Hz, 1H), 7.02 (q,

J=7.20 Hz, 1H), 7.01 (s, 1H), 6.77 (dd, *J*=0.49, 7.82 Hz, 1H), 3.94 (s, 3H), 2.31 (s, 3H), 2.00 (d, *J*=7.04 Hz, 3H). HRMS (ESI): m/z (M + H) calcd 421.1419; found 421.1440.

(*R*)-6-(1-(8-Fluoro-6-(3-methylisoxazol-5-yl)-[1,2,4]triazolo[4,3-*a*]pyridin-3-yl)ethyl)-3-(2-methoxyethoxy)-1,6-naphthyridin-5(6*H*)-one (19): Step 1: Coupling **9a** and **13c** in MeCN, 30 min, room temperature, 77% yield. LRMS (ESI): m/z (M + H) 483.2. Step 2: THF, 50 min, room temperature, 46% yield. The racemate was purified by supercritical fluid chromatography (SFC) by repeated 1.5 mL injections of a 5.6 mg/mL solution onto a Chiralpak AD-H, 2 cm x 15 cm (i.d. x length) column, eluting with 25% MeOH w/ 0.2% Et_2NH and 75% CO_2 at a flow rate of 75 mL/min to provide 133 mg peak 1 (***ent*-19**) with *ee* > 99% and 112 mg peak 2 (**19**) with *ee* > 99%.[29] ^{1}H NMR (400 MHz, CHLOROFORM-*d*) δ 8.73 (s, 1H), 8.72 (d, *J*=5.00 Hz, 1H), 8.15 (d, *J*=2.93 Hz, 1H), 7.42 (d, *J*=7.73 Hz, 1H), 7.29 (dd, *J*=0.98, 10.07 Hz, 1H), 7.08 (q, *J*=7.11 Hz, 1H), 6.83 (d, *J*=7.73 Hz, 1H), 6.43 (s, 1H), 4.29-4.37 (m, 2H), 3.82-3.88 (m, 2H), 3.49 (s, 3H), 2.39 (s, 3H), 2.17 (d, *J*=7.04 Hz, 3H). HRMS (ESI): m/z (M + H) calcd 465.1681; found 465.1695.

(*R*)-3-(2-Methoxyethoxy)-6-(1-(6-(3-methylisoxazol-5-yl)-[1,2,4]triazolo[4,3-*a*]pyridin-3-yl)ethyl)-1,6-naphthyridin-5(6*H*)-one (20): Step 1: Coupling **9b** and **13c** in MeCN, 2 h, room temperature, 23% yield. LRMS (ESI): m/z (M + H) 465.3. Step 2: THF, 1 h, room temperature, 73% yield. The racemate was purified by supercritical fluid chromatography (SFC) by repeated 1.0 mL injections of a 7 mg/mL solution onto a Chiralcel OD-H, 2 cm x 25 cm (i.d. x length) column, eluting with 35% MeOH w/ 0.2% Et_2NH and 65% CO_2 at a flow rate of 80 mL/min to provide 13 mg peak 1 (**20**) with *ee* > 99% and 14 mg peak 2 (***ent*-20**) with *ee* = 99%.[29] ^{1}H NMR (400 MHz, DMSO-d_6) δ 8.89 (t, *J*=1.27 Hz, 1H), 8.68 (d, *J*=3.03 Hz, 1H), 8.01 (dd, *J*=0.44, 2.98 Hz, 1H), 7.96 (dd, *J*=1.03, 9.63 Hz, 1H), 7.79 (dd, *J*=1.66, 9.59 Hz, 1H), 7.60 (d, *J*=7.83 Hz, 1H), 6.99 (s, 1H), 7.02 (q, *J*=7.10 Hz, 1H), 6.75 (dd, *J*=0.39, 7.73 Hz, 1H), 4.27-4.34 (m, 2H), 3.68-3.74 (m, 2H), 3.32 (s, 3H), 2.31 (s, 3H), 1.99 (d, *J*=7.04 Hz, 3H). HRMS (ESI): m/z (M + H) calcd 447.1775; found 447.1783. The solid was recrystallization in EtOH to form crystal anhydrous free base form I or form II, with a melting point of 181.4 and 181.2 °C, respectively.

(*R*)-6-(1-(8-Fluoro-6-(1-methyl-1*H*-pyrazol-4-yl)-[1,2,4]triazolo[4,3-*a*]pyridin-3-yl)ethyl)-1,6-naphthyridin-5(6*H*)-one (21): Step 1: Coupling **9c** and **13a** in MeCN, 30 min, 0 °C, 67% yield. LRMS (ESI): m/z (M + H) 408.2. Step 2: THF, 50 min, room temperature, 58% yield. The racemate was purified by supercritical fluid chromatography (SFC) by repeating 1.25 mL injections of a 5 mg/mL solution onto a Chiralcel OJ-H, 2 cm x 15 cm (i.d. x length) column, eluting with 20% MeOH w/ 0.2% Et_2NH and 80% CO_2 at a flow rate of 70 mL/min to provide 60 mg peak 1 (**21**) with *ee* > 99% and 41 mg peak 2 (***ent*-21**) with *ee* > 99%.[29] ^{1}H NMR (400 MHz, CHLOROFORM-*d*) δ 8.92 (dd, *J*=1.86, 4.70 Hz, 1H), 8.82 (dd, *J*=1.27, 8.12 Hz, 1H), 8.32 (d, *J*=1.17 Hz, 1H), 7.71 (d, *J*=0.88 Hz, 1H), 7.61 (d, *J*=0.29 Hz, 1H), 7.58 (d, *J*=7.83 Hz, 1H), 7.50 (dd, *J*=4.69, 8.12 Hz, 1H), 7.10 (dd, *J*=1.22, 10.61 Hz, 1H), 7.04 (q, *J*=7.08 Hz, 1H), 6.88 (d, *J*=7.92 Hz, 1H), 3.97 (s, 3H), 2.16 (d, *J*=7.14 Hz, 3H). HRMS (ESI): m/z (M + H) calcd 390.1473; found 390.1490.

(*R*)-6-(1-(8-Fluoro-6-(1-methyl-1*H*-pyrazol-4-yl)-[1,2,4]triazolo[4,3-*a*]pyridin-3-yl)ethyl)-3-methoxy-1,6-naphthyridin-5(6*H*)-one (22): Step 1: Coupling **9c** and **13b** in MeCN, 1 h, room temperature, 59% yield. LRMS (ESI): m/z (M + H) 437.8. Step 2: THF, 1 h, room temperature, 20% yield. The racemate e was purified by supercritical fluid chromatography (SFC) by repeating 0.3 mL injections of a 13 mg/mL solution onto a Chiralcel OD-H, 2 cm x 25 cm (i.d. x length) column, eluting with 35% EtOH w/ 0.2% Et_2NH and 65% CO_2 at a flow rate of 70 mL/min to provide 27 mg peak 1 (**22**) with *ee* > 99% and 27 mg peak 2 (***ent*-22**) (*ee* > 99%).[29] ^{1}H NMR (400 MHz, DMSO-d_6) δ 8.68 (d, *J*=3.03 Hz, 1H), 8.48 (d, *J*=1.08 Hz, 1H), 8.18 (d, *J*=0.39 Hz, 1H), 7.99 (dd, *J*=0.54, 3.08 Hz, 1H), 7.85 (d, *J*=0.78 Hz, 1H), 7.67 (dd, *J*=1.27, 12.13 Hz, 1H), 7.62 (d, *J*=7.54 Hz, 1H), 6.94 (q, *J*=7.10 Hz, 1H), 6.77 (dd, *J*=0.44, 7.78 Hz, 1H), 3.94 (s, 3H), 3.89 (s, 3H), 1.99 (d, *J*=7.14 Hz, 3H). HRMS (ESI): m/z (M + H) calcd 420.1597; found 420.1579.

(*R*)-6-(1-(8-Fluoro-6-(1-methyl-1*H*-pyrazol-4-yl)-[1,2,4]triazolo[4,3-*a*]pyridin-3-yl)ethyl)-3-(2-methoxyethoxy)-1,6-naphthyridin-5(6*H*)-one (23): Step 1: Coupling **9c** and **13c** in MeCN, 30 min, room

temperature, 86% yield. LRMS (ESI): m/z (M + H) 482.2. Step 2: THF, 50 min, room temperature, 48% yield. The racemate was purified by supercritical fluid chromatography (SFC) by repeating 0.75 mL injections of a 30 mg/mL solution onto a Chiralpak AS-H, 2 cm x 15 cm (i.d. x length) column, eluting with 20% *i*-PrOH and 80% CO_2 at a flow rate of 50 mL/min to provide 120 mg peak 1 (**23**) with *ee* > 99% and 150 mg peak 2 (***ent*-23**) with *ee* > 99%.[29] ^{1}H NMR (400 MHz, CHLOROFORM-*d*) δ 8.72 (d, *J*=2.93 Hz, 1H), 8.31 (d, *J*=0.78 Hz, 1H), 8.15 (d, *J*=2.84 Hz, 1H), 7.72 (s, 1H), 7.61 (s, 1H), 7.42 (d, *J*=7.82 Hz, 1H), 7.09 (dd, *J*=0.73, 10.61 Hz, 1H), 7.05 (q, *J*=7.00 Hz, 1H), 6.82 (d, *J*=7.82 Hz, 1H), 4.26-4.37 (m, 2H), 3.97 (s, 3H), 3.80-3.88 (m, *J*=3.80, 5.10 Hz, 2H), 3.49 (s, 3H), 2.15 (d, *J*=7.14 Hz, 3H). HRMS (ESI): m/z (M + H) calcd 464.1859; found 464.1841. The solid was recrystallized in EtOH followed by addition of H_2O to form crystalline free base monohydrate form I, with a dehydration event at 40-55 °C, followed by a melt at 151-153 °C. The solid could be also recrystallization in EtOH under anhydrous conditions to form crystalline anhydrous free base form I with a melting point of 151-153 °C.

(*R*)-3-Methoxy-6-(1-(6-(1-methyl-1*H*-pyrazol-4-yl)-[1,2,4]triazolo[4,3-*a*]pyridin-3-yl)ethyl)-1,6-naphthyridin-5(6*H*)-one (24): Step 1: Coupling **9d** and **13b** in DMF, 1 h, room temperature, 63% yield. LRMS (ESI): m/z (M + H) 420.0. Step 2: THF, 2 h, room temperature, 40% yield. The racemate was purified by supercritical fluid chromatography (SFC) by repeating 3 mL injections of an 8.5 mg/mL solution onto a Chiralcel OD-H, 2 cm x 15 cm, (i.d. x length) column, eluting with 40% MeOH w/ 0.2% Et_2NH and 60% CO_2 at a flow rate of 70 mL/min to provide 84 mg peak 1 (**24**) with *ee* > 99% and 85 mg peak 2 (***ent*-24**) *ee* > 99%.[29] ^{1}H NMR (400 MHz, DMSO-d_6) δ 8.68 (d, *J*=3.03 Hz, 1H), 8.54 (s, 1H), 8.15 (s, 1H), 8.01 (d, *J*=2.84 Hz, 1H), 7.83 (dd, *J*=0.93, 9.54 Hz, 1H), 7.81 (d, *J*=0.68 Hz, 1H), 7.64 (dd, *J*=1.56, 9.49 Hz, 1H), 7.57 (d, *J*=7.82 Hz, 1H), 6.96 (q, *J*=7.04 Hz, 1H), 6.75 (d, *J*=7.73 Hz, 1H), 3.94 (s, 3H), 3.89 (s, 3H), 1.99 (d, *J*=7.04 Hz, 3H). HRMS (ESI): m/z (M + H) calcd 402.1685; found 402.1673.

(*R*)-3-(2-Methoxyethoxy)-6-(1-(6-(1-methyl-1*H*-pyrazol-4-yl)-[1,2,4]triazolo[4,3-*a*]pyridin-3-yl)ethyl)-1,6-naphthyridin-5(6*H*)-one (25): Step 1: Coupling **9d** and **13c** in MeCN, 30 min, room temperature, 54% yield. LRMS (ESI): m/z (M + H) 464.2. Step 2: THF, 50 min, room temperature, 21% yield. The racemate

was purified by supercritical fluid chromatography (SFC) by repeating 0.2 mL injections of a 42 mg/mL solution onto a Chiralcel OD-H, 2 cm x 25 cm (i.d. x length) column, eluting with 30% MeOH w/ 0.2% Et_2NH and 70% CO_2 at a flow rate of 70 mL/min to provide 38 mg peak 1 (**25**) with *ee* > 99% and 42 mg peak 2 (***ent*-25**) with *ee* = 96.7%.[29] ^{1}H NMR (400 MHz, DMSO-d_6) δ 8.69 (d, *J*=3.03 Hz, 1H), 8.55 (t, *J*=1.27 Hz, 1H), 8.16 (s, 1H), 8.03 (d, *J*=3.03 Hz, 1H), 7.84 (dd, *J*=1.17, 9.49 Hz, 1H), 7.81 (d, *J*=0.78 Hz, 1H), 7.64 (dd, *J*=1.56, 9.49 Hz, 1H), 7.57 (d, *J*=7.73 Hz, 1H), 6.96 (q, *J*=7.14 Hz, 1H), 6.75 (d, *J*=7.53 Hz, 1H), 4.28-4.33 (m, 2H), 3.89 (s, 3H), 3.69-3.74 (m, 2H), 3.32 (s, 3H), 1.98 (d, *J*=7.14 Hz, 3H). HRMS (ESI): m/z (M + H) calcd 446.1953; found 446.1935.

Biology

Kinase Assay. IC_{50} measurements of inhibitor activity against the recombinant MET kinase domain were determined using homogenous time-resolved fluorescence using a gastrin peptide as substrate. Each reaction consists of 10 µL of an 8 nM phosphorylated MET kinase domain (WT or mutant), increasing concentrations of inhibitor in a volume of 1.6 µL and 48 µL of buffer (60 mM HEPES pH 7.4, 50 mM NaCl, 20 mM $MgCl_2$, 5 mM $MnCl_2$, 2 mM DTT, 0.1 mM Na_3VO_4, 0.05% BSA) for 30 minutes at room temperature. Twenty microliters (20 µL) of ATP and gastrin (final concentrations are 4 µM for ATP -2/3 of Km - and 1 µM for the biotinylated gastrin) in the same buffer are then added to the reaction in a final volume of 80 µL and incubated at room temperature for 60 minutes. Five microliters (5 µL) of the above reaction is then added to a reaction mixture containing 11 nM of streptavidin-allophycocyanin (S-APC) and 0.1 nM europium-labeled anti-phosphotyrosine antibody (Eu-PT66) in a final volume of 85 µL for 30 minutes at room temperature before data capture using a fluorescence plate reader.

Cell-based Assay. IC_{50} measurements of inhibitor activity on HGF-mediated MET autophosphorylation were determined in serum-starved PC-3 cells using a quantitative electrochemiluminescence immunoassay. PC-3 cells were plated in high glucose DMEM with 10% FBS at a density of 20,000 cells/well in 96-well plates. The next day, cells were starved in low glucose DMEM containing 0.1% BSA for 16 hours. Cells in

the starvation media were then treated with a 10-point serial dilution of the inhibitor for one hour at 37 °C followed by stimulation with 200 ng/mL of recombinant human HGF for 10 minutes at 37 °C. Cells were washed once with PBS and lysed (1% Triton X-100, 50 mM Tris pH 8.0, 100 mM NaCl, Na_3VO_4 and protease inhibitors). Cell lysates were then used to measure the levels of MET phosphorylation using a quantitative assay as follows: a biotinylated antibody against MET (R&D Systems #BAF358) was pre-incubated with streptavidin beads (IGEN #110029) for 30 minutes at room temperature with rotation. Cell lysates (25 µL) were then added to 25 µL of biotin labeled anti-MET antibodies for 1 hour at room temperature with shaking. An antiphosphotyrosine antibody 4G10 (Upstate #05-321) (12.5 µL) was then added and allowed to incubate for 1 hour at room temperature followed by the addition of 12.5 µL of an ORI-Tag-labeled anti-mouse IgG (IGEN #110087) for 30 minutes at room temperature. PBS (175 µL) was then added to each reaction and levels of MET phosphorylation were measured using an IGEN instrument (Biomek FX). The IC_{50} values are calculated using Xlfit4-parameter equation.

Pharmacodynamic Assay. A single oral dose of compound **5, 19, 20 and 23** at 10 mg/kg was administered by oral gavage at 1, 3, 6, 9, 12 or 24 hours prior to euthanasia. MET phosphorylation was induced in the livers of female Balb/c mice by injection of 12 µg of human recombinant HGF *iv* 5 minutes prior to euthanasia. Levels of MET phosphorylation were determined by an electrochemiluminescent immunoassay. Data represents the mean +/- standard deviation (n=3). Statistical significance was determined by ANOVA followed by Bonferroni/Dunn post hoc test. * = $p<0.0001$ compared to HGF control. Red circles represent the mean terminal unbound concentration in the plasma +/- standard deviation (n=3). Work was conducted in an AALAC accredited facility with IACUC approved protocols.

Xenograft Assay. The cells were maintained at 37°C in DMEM high glucose culture medium (Gibco/BRL, Grand Island,NY) supplemented with 10% FBS (Hyclone, Logan, Utah) and 1% PSG (Gibco/BRL). TPR-Met cells were determined to be free of contamination with mycoplasma as well as a panel of murine viral pathogens. 72 female CD-1 nude mice from Charles River Laboratories were injected with 1 $x10^6$ TPR-Met cells in 0.2 ml of DMEM (no FBS & no PSG) subcutaneously in the right flank. Compound **23** was

administered by oral gavage once per day beginning 24 hours post tumor cell implantation (NIH3T3 cells transfected with human TPR-Met). Results are expressed as mean ± standard error (n = 12 per group). Asterisk denotes p <0.0005 compared to treatment with vehicle. Vehicle: 20% HPBCD, pH 3.5 adjusted with methanesulfonic acid. Work was conducted in an AALAC accredited facility with IACUC approved protocols.

Crystallization of c-Met complexes. The kinase domain of c-Met (residues 1048–1350) was expressed, purified, and crystallized as described previously.[30] Diffraction data were collected on a FR-E rotating anode X-ray source equipped with an RAXIS IV++ detector and images were processed using the HKL suite of programs.[31] The structures were solved by molecular replacement with AMORE and they were refined using REFMAC.[32] Model building was performed with COOT.[33]

ASSOCIATED CONTENT

Supporting Information

Crystallographic data collection and refinement statistics and the cocrystal structure for **5** (PDB code 5EYC) and **23** (PDB code 5EYD) with MET. Molecular formula strings spreadsheet. This material is available free of charge via the Internet at http://pubs.acs.org.

AUTHOR INFORMATION

Corresponding Author

Alessandro A. Boezio

*Phone: 617-444-5104. Fax: 617-621-3908. E-mail: aboezio@amgen.com.

Notes: The authors declare no competing financial interest.

ACKNOWLEDGMENTS

The authors are grateful to Michael Zhang and Yajing Yang for enzyme and cell assay support, Loren Berry for in vitro PKDM analysis, Larry Miller and Matt Potter for chiral separation of products bearing

stereogenic centers, Kristin Andrews for generating Figure 3 from MOE software and Jie Yan and John Stellwagen for compound synthesis.

ABBREVIATIONS USED

CYP3A4, cytochrome P450 3A4; Cl, clearance; Cl_u, unbound clearance; f_u, unbound fraction; HATU, (1-[Bis(dimethylamino)methylene] 1*H*-1,2,3-triazolo[4,5-*b*]pyridinium 3-oxid hexafluorophosphate); HGF, hepatocyte growth factor; HLM, human liver microsomes; HPBCD, hydroxypropyl-β-cyclodextrin; LCMS, liquid chromatography mass spectrometry; LRMS, low resolution mass spectrometry; MET, mesenchymal epithelial transition factor; MLM, mouse liver microsomes; RLM, rat liver microsomes; SIF, simulated intestinal fluid; $T_{1/2}$, half-life; TDI, time-dependent inhibition; V_{ss}, volume of distribution; X-Phos, dicyclohexylphosphino-2′,4′,6′-triisopropylbiphenyl

References

1) Giordano, S.; Ponzetto, C.; Di Renzo, M. F.; Cooper, C. S.; Comoglio, P. M. Tyrosine kinase receptor indistinguishable from the c-met protein. *Nature* **1989**, *339*, 155–156.

2) Gherardi, E.; Birchmeier, W.; Birchmeier, C.; Vande Woude, G. Targeting MET in cancer: rationale and progress. *Nat. Rev. Cancer* **2012**, *12*, 89−103.

3) Dharmawardana, P. G.; Giubellino, A.; Bottaro, D. P. Hereditary papillary renal carcinoma type I. *Curr. Mol. Med.* **2004**, *4*, 855–868.

4) Cui, J. J. Targeting receptor tyrosine kinase MET in cancer: small molecule inhibitors and clinical progress. *J. Med. Chem.* **2014**, *57*, 4427−4453.

5) Porter, J. Small molecule c-Met kinase inhibitors: a review of recent patents. *Expert Opin. Ther. Pat.* **2010**, *20*, 159−177.

6) (a) Liu, L.; Siegmund, A.; Xi, N.; Kaplan-Lefko, P.; Rex, K.; Chen, A.; Lin, J.; Moriguchi, J.; Berry, L.; Huang, L.; Teffera, Y.; Yang, Y.; Zhang, Y.; Bellon, S. F.; Lee, M.; Shimanovich, R.; Bak, A.; Dominguez, C.; Norman, M. H.; Harmange, J.-C.; Dussault, I.; Kim, T.-S. Discovery of a potent, selective, and orally bioavailable c-Met inhibitor: 1-(2-hydroxy-2-methylpropyl)-*N*-(5-(7-methoxyquinolin-4-yloxy)pyridin-2-yl)-5-methyl-3-oxo-2-phenyl-2,3-dihydro-1*H* pyrazole-4-carboxamide (AMG 458). *J. Med. Chem.* **2008**, *51*, 3688−3691. (b) Liu, L.; Norman, M. H.; Lee, M.; Xi, N.; Siegmund, A.; Boezio, A. A.; Booker, S.; Choquette, D.; D'Angelo, N. D.; Germain, J.; Yang, K.; Yang, Y.; Zhang, Y.; Bellon, S. F.; Whittington, D. A.; Harmange, J.-C.; Dominguez, C.; Kim, T. S.; Dussault, I. Structure-based design of novel class II c-Met inhibitors: 2. SAR and kinase selectivity profiles of the pyrazolone series. *J. Med. Chem.* **2012**, *55*, 1868−1897. (c) Norman, M. H.; Liu, L.; Lee, M.; Xi, N.; Fellows, I.; D'Angelo, N. D.; Dominguez, C.; Rex, K.; Bellon, S. F.; Kim, T.-S.; Dussault, I. Structure-based design of novel class II c-Met inhibitors: 1. Identification of pyrazolone-based derivatives. *J. Med. Chem.* **2012**, *55*, 1858−1867.

7) Albrecht, B. K.; Harmange, J.-C.; Bauer, D.; Berry, L.; Bode, C.; Boezio, A. A.; Chen, A.; Choquette, D.; Dussault, I.; Fridrich, C.; Hirai, S.; Hoffman, D.; Larrow, J. F.; Kaplan-Lefko, P.; Lin, J.; Lohman, J.; Long, A. M.; Moriguchi, J.; O'Connor, A.; Potashman, M. H.; Reese, M.; Rex, K.; Siegmund, A.; Shah, K.; Shimanovich, R.; Springer, S. K.; Teffera, Y.; Yang, Y.; Zhang, Y.; Bellon, S. Discovery and optimization of triazolopyridazines as potent and selective inhibitors of the c-Met kinase. *J. Med. Chem.* **2008**, *51*, 2879−2882.

8) Boezio, A. A.; Berry, L.; Albrecht, B. K.; Bauer, D.; Bellon, S. F.; Bode, C.; Chen, A.; Choquette, D.; Dussault, I.; Hirai, S.; Kaplan-Lefko, P.; Larrow, J. F.; Lin, M. H.; Lohman, J.; Potashman, M. H.; Rex, K.; Santostefano, M.; Shah, K.; Shimanovich, R.; Springer, S. K.; Teffera, Y.; Yang, Y.; Zhang, Y.; Harmange, J.-C. Discovery and optimization of potent and selective triazolopyridazine series of c-Met inhibitors. *Bioorg. Med. Chem. Lett.* **2009**, *19*, 6307−6312.

9) Bode, C. M.; Boezio, A. A.; Albrecht, B. K.; Bellon, S. F.; Berry, L.; Broome, M. A.; Choquette, D.; Dussault, I.; Lewis, R. T.; Lin, M.-H. J.; Rex, K.; Whittington, D. A.; Yang, Y.; Harmange, J.-C. Discovery

and optimization of a potent and selective triazolopyridinone series of c-Met inhibitors. *Bioorg. Med. Chem. Lett.* **2012**, *22*, 4089−4093.

10) Peterson, E. A.; Teffera, Y.; Albrecht, B. K.; Bauer, D.; Bellon, S. F.; Boezio, A.; Boezio, C.; Broome, M. A.; Choquette, D.; Copeland, K. W.; Dussault, I.; Lewis, R.; Lin, M.-H. J.; Lohman, J.; Liu, J.; Potashman, M.; Rex, K.; Shimanovich, R.; Whittington, D. A.; Vaida, K. R.; Harmange, J.-C. Discovery of potent and selective 8-fluorotriazolopyridine c-Met inhibitors. *J. Med. Chem.* **2015**, *58*, 2417−2430.

11) (a) Bio, M.; Fang, E.; Milne, J. E.; Wiedemann, S.; Wilsily, A. Method for the preparation of (1,2,4)-triazolo[4,3-*a*]pyridines. PCT Int. Appl. December 31, 2014, WO 2014210042 A2 20141231. (b) Albrecht, B. K.; Bauer, D.; Bellon, S.; Bode, C. M.; Booker, S.; Boezio, A.; Choquette, D.; D'Amico, E.; Harmange, J.-C.; Hirai, S.; Hungate, R. W.; Kim, T.-S.; Lewis, R. T.; Liu, L.; Lohman, J.; Norman, M. H.; Potashman, M.; Siegmund, A. C.; Springer, S.; Stec, M.; Xi, N.; Yang, K.; Peterson, E. A.; Romero, K.; Copeland, K. W. Fused heterocyclic derivatives and method of use as c-met inhibitors. PCT Int. Appl. July 23, 2009, WO 2009091374 A2 20090723.

12) Zhou, S.; Chan, S. Y.; Goh, B. C.; Chan, E.; Duan, W.; Huang, M.; McLeod, H. L. Mechanism-based inhibition of cytochrome P450 3A4 by therapeutic drugs. *Clin. Pharmacokinet.* **2005**, *44*, 279–304.

13) (a) Edwards, M. P.; Price, D. A. Role of physicochemical properties and ligand lipophilicity efficiency in addressing drug safety risks. *Ann. Reports Med. Chem.* **2010**, *45*, 381–391. (b) Freeman-Cook, K. D.; Hoffman, R. L.; Johnson, T. W. Lipophilic efficiency: the most important efficiency metric in medicinal chemistry. *Future Med. Chem.* **2013**, *5*, 113–115. (c) Shultz, M. D. Setting expectations in moleculare optimizations: strengths and limitations of commonly used composite parameter. *Bioorg. Med. Chem. Lett.* **2013**, *23*, 5980–5991. (d) Shultz, M. D. The thermodynamic basis for the use of lipophilic efficiency (LipE) in enthalpic optimizations. *Bioorg. Med. Chem. Lett.* **2013**, *23*, 5992–6000.

14) Lipophilic-efficiency metrics are reported for purpose of retrospective analysis of this work.

15) For a discussion of the relationship between MET target coverage and tumor growth inhibition, see: Yamazaki, S.; Skaptason, J.; Romero, D.; Lee, J. H. Zou, H. Y.; Christensen, J. G.; Koup, J. R.; Smith, B.

J.; Koudriakova, T. Pharmacokinetic-pharmacodynamic modeling of biomarker response and tumor growth inhibition to an orally available cMet kinase inhibitor in human tumor xenograft mouse models. *Drug Met. Disp.* **2008**, *36*, 1267–1274.

16) Potency of the (*S*)-enantiomer (MET Biochemical IC_{50}: 963 nM, Cellular IC_{50}: 2630 nM).

17) For alternative route of synthesis of **5**, see: Fang, Y.-Q.; Bio, M. M.; Hansen, K. B.; Potter, M. S.; Clausen, A. Magnesium coordination-directed *N*-selective stereospecific alkylation of 2-pyridones, carbamates, and amides using α-halocarboxylic acids. *J. Am. Chem. Soc.* **2010**, *132*, 15525–15527.

18) Although this exact asymmetric synthesis was efficient, other derivatives often led to degradation of *ee* upon amide coupling.

19) PDB deposition code number for the crystal structure of MET + **5** is 5EYC. Additional, PDB deposition code number for the crystal structure of MET + **23** is 5EYD).

20) Molecular Operating Environment (MOE), 2014.09; Chemical Computing Group Inc., 1010 Sherbrooke St. West, Suite #910, Montreal, QC, Canada, H3A 2R7, **2014**.

21) See Scheme 1 for atom numbering.

22) The absolute stereochemistry was assigned by crystallization of enantiopure **24** with unphosphorylated MET and confirmed from chiral synthesis (see Scheme 2).

23) Balogh, M.; Hermecz, I.; Naray-Szabo, G.; Simon, K.; Meszaros, Z. Studies on naphthyridines. An unexpected product in Hantzsch pyridine synthesis. *J. Chem. Soc., Perkin Trans. 1*, **1986**, *5*, 753–757.

24) The stereochemistry of **18-25** was made based on potency and in analogy to the known potent enantiomer of **5**.

25) See reference 10 for comparable results.

26) (a) Zhang, Y; Kaplan-Lefko, P. J.; Rex, K.; Yang, Y.; Moriguchi, J.; Osgood, T.; Mattson, B.; Coxon, A.; Reese, M.; Kim, T.-S.; Lin, J.; Chen, A.; Burgess, T. L.; Dussault, I. Identification of a novel recepteur d'origine Nantais/c-Met small-molecule kinase inhibitor with antitumor activity in vivo. *Cancer Res.* **2008**, *68*, 6680–6687. (b) Park, M.; Dean, M.; Cooper, C. S.; Schmidt, M.; O'Brien, S. J.; Blaire, D. G.; Vande Woude, G. F. Mechanism of met oncogene activation. *Cell* **1986**, *45*, 895–904.

27) *KINOMEscan*™. At a concentration of 1 μM, compound **23** binds to MET (3.1% POC) and no other kinases < 50% POC).

28) Racemization was observed at higher temperature.

29) On the basis of previous crystallographic data and potency recorded for related compound in the same program, the absolute stereochemistry has been assigned to be the (*R*) enantiomer.

30) Bellon, S. F.; Kaplan-Lefko, P.; Yang, Y.; Zhang, Y.; Moriguchi, J.; Rex, K.; Johnson, C. W.; Rose, P. E.; Long, A. M.; O'Connor, A. B.; Gu, Y.; Coxon, A.; Kim, T.-S.; Tasker, A.; Burgess, T. L.; Dussault, I. c-Met inhibitors with novel binding mode show activity against several hereditary papillary renal cell carcinoma-related mutations. *J. Biol. Chem.* **2008**, *283*, 2675–2683.

31) Otwinowski, Z.; Minor, W. Processing of X-ray diffraction data collected in oscillation mode. *Methods Enzymol.* **1997**, *276*, 307–326.

32) (a) Navaza, J. *AMoRe*: an automated package for molecular replacement. *Acta Crystallogr. A* **1994**, *50*, 157-163. (b) Murshudov, G.N.; Vagin, A.A.; Dodson, E. J. Refinement of macromolecular structures by the maximum-likelihood method. *Acta Crystallogr.* **1997**, *D53*, 240–255.

33) Emsley, P.; Cowtan, K. *Coot*: model-building tools for molecular graphics. *Acta Crystallogr*. **2004**, *D60*, 2126–2132.

TABLE OF CONTENTS GRAPHIC